© 2021. Published by The Company of Biologists Ltd | Journal of Experimental Biology (2021) 224, jeb240960. doi:10.1242/jeb.240960

RESEARCH ARTICLE

Dramatic changes in mitochondrial substrate use at critically high temperatures: a comparative study using *Drosophila*

Lisa Bjerregaard Jørgensen[1,*], Johannes Overgaard[1], Florence Hunter-Manseau[2] and Nicolas Pichaud[2]

ABSTRACT

Ectotherm thermal tolerance is critical to species distribution, but at present the physiological underpinnings of heat tolerance remain poorly understood. Mitochondrial function is perturbed at critically high temperatures in some ectotherms, including insects, suggesting that heat tolerance of these animals is linked to failure of oxidative phosphorylation (OXPHOS) and/or ATP production. To test this hypothesis, we measured mitochondrial oxygen consumption rate in six *Drosophila* species with different heat tolerance using high-resolution respirometry. Using a substrate–uncoupler–inhibitor titration protocol, we examined specific steps of the electron transport system to study how temperatures below, bracketing and above organismal heat limits affect mitochondrial function and substrate oxidation. At benign temperatures (19 and 30°C), complex I-supported respiration (CI-OXPHOS) was the most significant contributor to maximal OXPHOS. At higher temperatures (34, 38, 42 and 46°C), CI-OXPHOS decreased considerably, ultimately to very low levels at 42 and 46°C. The enzymatic catalytic capacity of complex I was intact across all temperatures and accordingly the decreased CI-OXPHOS is unlikely to be caused directly by hyperthermic denaturation/inactivation of complex I. Despite the reduction in CI-OXPHOS, maximal OXPHOS capacity was maintained in all species, through oxidation of alternative substrates – proline, succinate and, particularly, glycerol-3-phosphate – suggesting important mitochondrial flexibility at temperatures exceeding the organismal heat limit. Interestingly, this failure of CI-OXPHOS and compensatory oxidation of alternative substrates occurred at temperatures that correlated with species heat tolerance, such that heat-tolerant species could defend 'normal' mitochondrial function at higher temperatures than sensitive species. Future studies should investigate why CI-OXPHOS is perturbed and how this potentially affects ATP production rates.

KEY WORDS: Complex I, Mitochondrial flexibility, Glycerol-3-phosphate dehydrogenase, Substrate control, Thermal sensitivity, Thermal tolerance

INTRODUCTION

The body temperature of ectotherms is closely associated with the temperature of their environment. Accordingly, organismal resistance to temperature effects, i.e. thermal tolerance, is an important trait in shaping the biogeographic distribution of ectotherm species, including insects (Addo-Bediako et al., 2000; Kellermann et al., 2012; Sunday et al., 2019). With projections of increasing average temperatures as well as the frequency and intensity of extreme temperature events through climate change (IPCC, 2014), much effort has been put into using characterization of species heat tolerance to predict global changes in species distribution (Kingsolver et al., 2013; Sunday et al., 2012). Yet, the physiological shortcomings underlying the loss of function and mortality associated with heat stress are still not fully understood for insects (for reviews, see Bowler, 2018; González-Tokman et al., 2020; Neven, 2000).

Some physiological and cellular mechanisms often listed as potential contributors to heat mortality in insects and other ectotherms are inactivation and denaturation of proteins, temperature effects on membrane organization, unaligned temperature sensitivities (Q_{10}) of coupled biochemical reactions as well as insufficient oxygen supply in line with mismatched ATP demand and supply (Hochachka and Somero, 2002; Schmidt-Nielsen, 1990). For terrestrial insects, there is little evidence to suggest that deficient oxygen supply to the respiring cells is a cause of heat mortality (Klok, 2004; Mölich et al., 2013; Verberk et al., 2015). For example, it is rarely found that moderate hypoxia or hyperoxia alters heat tolerance as would be expected by the oxygen- and capacity-limited thermal tolerance (OCLTT) hypothesis (see Verberk et al., 2015). However, this general finding does not exclude the possibility that exposure to extreme temperatures challenges mitochondrial function and their ability to produce ATP via oxidative phosphorylation (OXPHOS), which is also discussed in a recent review of the literature on mitochondria and ectotherm thermal limits (Chung and Schulte, 2020).

Metabolic demand increases with temperature and to maintain cellular homeostasis the rate of mitochondrial aerobic respiration must keep pace (Blier et al., 2014; Schulte, 2015). Accordingly, thermal sensitivity of mitochondria has been suggested to be important for thermal tolerance, and thermal adaptation of mitochondrial functions has been observed in several ectothermic phyla (Chung et al., 2018; Ekström et al., 2017; Fangue et al., 2009; Harada et al., 2019; Havird et al., 2020; Hraoui et al., 2020; Hunter-Manseau et al., 2019; Iftikar et al., 2010, 2014; Kake-Guena et al., 2017; Martinez et al., 2016; see also Chung and Schulte, 2020). Most mitochondrial studies addressing the effects of high temperature in ectotherms have focused on aquatic invertebrates or fish, while only a few studies have used insects, even though they comprise >70% of all animal species (Stork, 2018) and have the most rapidly contracting muscles in nature (Beenakkers et al., 1984; Candy et al., 1997; but see Chamberlin, 2004; Pichaud et al., 2010, 2011, 2012, 2013; and references below for studies on insect mitochondrial function). In insect flight muscle, mitochondrial respiration and ATP turnover may increase 100-fold when transitioning from rest to flight (Davis and Fraenkel, 1940; Krogh and Weis-Fogh, 1951; Weis-Fogh, 1964), and up to 20-fold in *Drosophila* (Chadwick and Gilmour, 1940). Hence, to sustain this intense activity, insect flight muscle metabolism must be extremely flexible. To our knowledge the most comprehensive investigation of

[1]Zoophysiology, Department of Biology, Aarhus University, 8000 Aarhus C, Denmark. [2]Department of Chemistry and Biochemistry, Université de Moncton, Moncton, NB, Canada, E1A 3E9.

*Author for correspondence (lbj@bio.au.dk)

L.B.J., 0000-0002-4438-4558; J.O., 0000-0002-2851-4551; F.H.-M., 0000-0001-5251-807X; N.P., 0000-0002-2820-8124

Received 23 November 2020; Accepted 21 January 2021

Journal of Experimental Biology (2021) 224, jeb240960. doi:10.1242/jeb.240960

List of abbreviations

Acetyl-CoA	acetyl coenzyme A
ADP	adenosine diphosphate
asc	ascorbate
ATP	adenosine triphosphate
cG3PDH	cytoplasmic glycerol-3-phosphate dehydrogenase
CI	complex I (NADH:ubiquinone oxidoreductase)
CII	complex II (succinate dehydrogenase)
CIII	complex III (coenzyme Q:cytochrome *c* oxidoreductase)
CIV	complex IV (cytochrome *c* oxidase)
CS	citrate synthase
CT_{max}	critical thermal maximum
CV	complex V (ATP synthase)
Cyt *c*	cytochrome *c*
DHAP	dihydroxyacetone phosphate
ETS	electron transport system
$ETS_{max}/OXPHOS_{max}$	non-coupled ratio
$FADH_2$	flavin adenine dinucleotide
FCCP	carbonyl cyanide-4-(trifluoromethoxy)-phenylhydrazone
G3P	glycerol-3-phosphate
GAP	glyceraldehyde-3-phosphate
$j_{\approx P}$	OXPHOS coupling efficiency
LEAK	non-coupled (to phosphorylation) respiration
MPC	mitochondrial pyruvate carrier
mtG3PDH	mitochondrial glycerol-3-phosphate dehydrogenase
NADH	nicotinamide adenine dinucleotide
OCLTT	oxygen- and capacity-limited thermal tolerance
OXPHOS	oxidative phosphorylation
PDH	pyruvate dehydrogenase
P_i	inorganic phosphate
ProDH	proline dehydrogenase
Q	ubiquinone pool
ROS	reactive oxygen species
ROX	residual oxygen consumption
saz	sodium azide
SCR	substrate contribution ratio
TCA	tricarboxylic acid
TMPD	(*N*,*N*,*N*′,*N*′-tetramethyl-*p*-phenylenediamine)

the association between insect heat tolerance and mitochondrial function is a series of studies led by Bowler and co-workers on blowflies. Here, the authors described how flight muscle mitochondria isolated from blowflies that had been exposed to sublethal heat stress *in vivo* displayed impaired mitochondrial function (Bowler and Kashmeery, 1981; Davison and Bowler, 1971), and that the organismal recovery from heat exposure (indicated by regained flight ability) was closely associated with the restoration of mitochondrial respiration (Bowler and Kashmeery, 1979; Davison and Bowler, 1971). Similarly, increased organismal heat tolerance induced by a heat shock treatment was found to mitigate damage to mitochondrial function from subsequent sublethal heat stress both *in vivo* and *in vitro* (El-Wadawi and Bowler, 1995). Substantial evidence suggests that mitochondrial oxygen consumption continues beyond the thermal threshold of movement (CT_{max}) (Heinrich et al., 2017; Mölich et al., 2013), which is also supported by the blowfly studies, but an important conclusion is that the coupled reactions in mitochondria are challenged around the organismal heat limits (El-Wadawi and Bowler, 1996). Specifically, the study by El-Wadawi and Bowler (1996) on blowfly flight muscle indicated that complex I (CI) could be the site of mitochondrial heat damage following a sublethal heat exposure.

In a recent study, we characterized heat tolerance of 11 *Drosophila* species representing a wide array of ecotypes and found pronounced differences in species heat tolerance which was closely related to the temperature of their current distribution (Jørgensen et al., 2019). In the present study, we used a subset of this comparative system to ask: (1) whether and how high temperature affects mitochondrial function in *Drosophila* and (2) whether heat-induced changes in mitochondrial function are correlated with organismal heat tolerance. Previous studies on mitochondrial function and temperature relationships in *Drosophila* have focused on genetic components (mitochondrial haplotypes) and were measured at less stressful high temperatures (up to 28°C) where organismal function is easily maintained (Pichaud et al., 2010, 2011, 2012, 2013). In contrast, the present study examined effects of high temperature on the electron transport system (ETS) in six species of *Drosophila* representing low, intermediate and high heat tolerance at temperatures approaching and surpassing the lethal limit (19–46°C). This was examined in permeabilized thoraces using high-resolution respirometry to measure multiple steps of the ETS during OXPHOS and non-coupled respiration. To specifically address the role of CI as the site of heat damage (El-Wadawi and Bowler, 1996), we investigated whether complex I-supported OXPHOS (CI-OXPHOS) diminished at high temperatures, and examined whether other components of the ETS compensated for this under these circumstances, attesting to mitochondrial flexibility during heat stress in *Drosophila*. Finally, we measured *in vitro* activity of mitochondrial enzymes related to CI substrate oxidation (pyruvate dehydrogenase, citrate synthase and CI enzymatic activity) to examine whether changes in mitochondrial function were directly related to the collapse of protein function.

MATERIALS AND METHODS

Experimental animals

The present study used six species of *Drosophila* that we previously characterized with respect to heat tolerance (Jørgensen et al., 2019). The species are listed here in order of increasing level of heat tolerance and the temperature reported to cause knockdown after a 1 h exposure; *D. immigrans* Sturtevant 1921 (35.4°C); *D. subobscura* Collin 1936 (35.6°C); *D. mercatorum* Patterson and Wheeler 1942 (37.1°C); *D. melanogaster* Meigen 1830 (38.3°C); *D. virilis* Sturtevant 1916 (38.8°C) and *D. mojavensis* Patterson 1940 (41.2°C). Details on population origin can be found in table 1 of Jørgensen et al. (2019). Flies were kept at Aarhus University (Aarhus, Denmark) for several years before shipping them to the Université de Moncton (Moncton, NB, Canada). Upon arrival, flies were acclimated to their previous environmental conditions for about 3 months prior to the start of experiments (i.e. allowing multiple generations before use). Specifically, flies were maintained at 19°C with a diurnal cycle (12 h:12 h light:dark) in 35 ml vials with approximately 15 ml oat-based Leeds medium (see Andersen et al., 2015). Parental flies were moved to a fresh vial every 5–7 days to avoid excessive egg density, and newly eclosed flies were transferred to fresh vials every 2–3 days. Only females 4–8 days post-eclosion were used for experiments.

Mitochondrial oxygen consumption in permeabilized thoraces

High-resolution respirometry was performed on permeabilized thoraces in the Oxygraph-O2K system (Oroboros Instruments, Innsbruck, Austria) using a protocol for *Drosophila* based on Simard et al. (2018). The steps for this protocol are outlined below.

Preparation of permeabilized thoraces

All steps of the permeabilization protocol were performed on ice. Initially, flies were incapacitated on ice and females were then transferred to a Petri dish where the thorax was separated from the head and abdomen. Wings and legs were then removed using a razor

blade and a pair of fine-tipped forceps. The number of thoraces required to achieve the target mass of 0.4–1 mg for each Oxygraph chamber was species specific, as size differs between species. For the larger species (*D. immigrans*, *D. subobscura*, *D. mercatorum* and *D. virilis*), two thoraces were used for each chamber, while three thoraces were prepared for the smaller *D. melanogaster* and *D. mojavensis*. Isolated thoraces were immediately transferred to a small Petri dish containing an ice-cold biological preservation solution (BIOPS; 2.77 mmol l^{-1} CaK_2EGTA, 7.23 mmol l^{-1} K_2EGTA, 5.77 mmol l^{-1} Na_2ATP, 6.56 mmol l^{-1} $MgCl_2$, 20 mmol l^{-1} taurine, 15 mmol l^{-1} Na_2phosphocreatine, 20 mmol l^{-1} imidazole, 0.5 mmol l^{-1} dithiothreitol, 50 mmol l^{-1} K-MES, pH 7.1). Thoraces were mechanically permeabilized by delicately poking the tissue with fine-tipped forceps, and the thoraces were then incubated in BIOPS supplemented with 62.5 µg ml^{-1} saponin (prepared daily) for 15 min on an orbital shaker (220 rpm) for chemical permeabilization. After 15 min, the thoraces were transferred to ice-cold respiration medium [RESPI; 120 mmol l^{-1} KCl, 5 mmol l^{-1} KH_2PO_4, 3 mmol l^{-1} Hepes, 1 mmol l^{-1} $MgCl_2$, 1 mmol l^{-1} EGTA, adjusted to pH 7.2, then 0.2% BSA (w/v) added], and incubated for 5 min on the orbital shaker (220 rpm) to wash out saponin. Prepared thoraces were gently dry-blotted on a Kimwipe to remove excess RESPI solution and weighed [Secura 225D-1s semi-micro balance (0.01 mg) or Cubis MSE6.6S-000-DM micro balance (0.001 mg), Sartorius, Göttingen, Germany] before they were returned to a droplet of RESPI medium placed on Parafilm over ice, such that each RESPI droplet contained the permeabilized thoraces for a single chamber.

Oxygen consumption rate

Mitochondrial oxygen consumption was measured at six different temperatures: 19°C (acclimation temperature), 30, 34, 38, 42 and 46°C to cover both benign and extreme temperatures for all species. The Oxygraph chambers were set to the assay temperature prior to air calibration, then filled with 2.3 ml RESPI medium and the stoppers were fully inserted to avoid air bubbles. Excess RESPI medium was aspirated, the stoppers were lifted using the spacer, and the system was allowed to equilibrate for at least 45 min (with stirring at 750 rpm) with the gas phase (air) and stabilize the oxygen concentration dissolved in the medium (solubility decreasing with increasing temperature). When the oxygen signal was stable (as per the recommended ±1 pmol O_2 s^{-1} ml^{-1}), the system was calibrated relative to the barometric and water vapour pressure (DatLab, version 6.1.0.7, Oroboros Instruments).

Once the Oxygraph had been calibrated, a general substrate–uncoupler–inhibitor titration (SUIT) protocol was employed to measure mitochondrial oxygen consumption at specific steps of the ETS. These steps are described below and are also outlined in Fig. 1, and will be referred to in parentheses throughout the description of the protocol. Concentrations reported here are calculated final concentrations in the 2 ml Oxygraph chamber. Measurements started by removing the chamber stopper and adding 10 mmol l^{-1} pyruvate (prepared daily) and 2 mmol l^{-1} malate (step 1) followed by the pre-weighed permeabilized thoraces. The oxygen concentration in the chamber was raised to ∼150–175% air-saturation to avoid any oxygen diffusion limitation in the tissue, and the chambers were closed. When oxygen consumption rate was stable, this was taken as the LEAK respiration at the level of complex I (CI-LEAK), which is a non-phosphorylating respiration rate. Injection of 5 mmol l^{-1} ADP (step 2) coupled the proton gradient created by electron transfer in CI to phosphorylation of ADP to ATP (CI-OXPHOS). The integrity of the mitochondrial outer membrane was then examined by injecting 10 µmol l^{-1} cytochrome *c* (step 3). A disrupted mitochondrial outer membrane would allow the native cytochrome *c*, which is loosely associated with the exterior of the inner mitochondrial membrane, to escape the intermembrane space and subsequently limit the electron transfer between complex III (CIII) and complex IV (CIV) (i.e. limiting oxygen consumption). Accordingly, an injection of cytochrome *c* that results in increased oxygen consumption indicates a compromised outer mitochondrial membrane (probably due to permeabilization), and preparations where oxygen consumption rate increased more than 15% were discarded from the analysis (Kuznetsov et al., 2008).

Three additional substrates were added to sequentially stimulate different parts of the ETS. First, 5 mmol l^{-1} proline was added as a substrate for proline dehydrogenase (ProDH, step 4) which transfers electrons to the Q-junction in the ETS (CI+ProDH-OXPHOS), followed by succinate (20 mmol l^{-1}, step 5), the substrate for complex II (CII; succinate dehydrogenase, CI+ProDH+CII-OXPHOS). Finally, *sn*-glycerol-3-phosphate (G3P, 15 mmol l^{-1}) was injected (step 6), which is directly oxidized by the mitochondrial glycerol-3-phosphate dehydrogenase (mtG3PDH, CI+ProDH+CII+mtG3PDH-OXPHOS) that similarly feeds electrons to the Q-junction (Fig. 1).

Non-coupled respiration in which the proton gradient produced by the ETS is not coupled to oxidative phosphorylation, and thus indicates the maximal capacity of the ETS, was achieved by titrating the uncoupler FCCP [carbonyl cyanide 4-(trifluoromethoxy)-phenylhydrazone, FCCP-ETS] in steps of 0.5–1 µmol l^{-1} (step 7). Next, the complexes of the ETS were inhibited by injecting 0.5 µmol l^{-1} rotenone (CI inhibitor, step 8), 5 mmol l^{-1} malonate (CII inhibitor, prepared daily, step 9) and 2.5 µmol l^{-1} antimycin A (CIII inhibitor, i.e. blocking the convergent electron transfer from the Q-junction, step 10) to measure the residual oxygen consumption (ROX). ROX was subtracted from all of the substrate-specific oxygen consumption rates to correct for oxygen used by non-mitochondrial oxidative side reactions (see Fig. S4).

The maximal capacity of CIV (cytochrome *c* oxidase) for reducing oxygen to water was measured by adding ascorbate (2 mmol l^{-1}) and the artificial substrate reducing cytochrome *c*, TMPD (*N*,*N*,*N*′,*N*,-tetramethyl-*p*-phenylenediamine, 0.5 mmol l^{-1}, step 11a). Shortly after the oxygen consumption rate had peaked, it started to decrease as a result of auto-oxidation of TMPD, and CIV was immediately inhibited by injection of sodium azide (20 mmol l^{-1}, step 11b). The maximal oxygen consumption rate of CIV was corrected for the underlying auto-oxidation of TMPD by adjusting the slope used to calculate oxygen consumption in DatLab (version 6.1.0.7, Oroboros Instruments).

This SUIT protocol typically took 50–55 min, from the time that the permeabilized thoraces were placed in the Oxygraph chambers to the signal stabilization after injection of the last inhibitor (sodium azide). All experiments described above were performed at Université de Moncton.

To examine the temperature sensitivity of electron transport through compartments of the ETS other than CI, a modified SUIT protocol was applied for additional measurements of oxygen consumption rate at 34 and 42°C. Here, CI was blocked with rotenone prior to injection of other substrates, and the CI substrates pyruvate and malate were omitted to minimize reverse electron transport through CI (Murphy, 2009). Accordingly, the following injections were made (concentrations identical to the general SUIT protocol); rotenone and succinate (CII-LEAK), ADP (CII-OXPHOS), cytochrome *c* (CIIc-OXPHOS), proline (CII+ProDH-OXPHOS), glycerol-3-phosphate (CII+ProDH+mtG3PDH-

Journal of Experimental Biology (2021) 224, jeb240960. doi:10.1242/jeb.240960

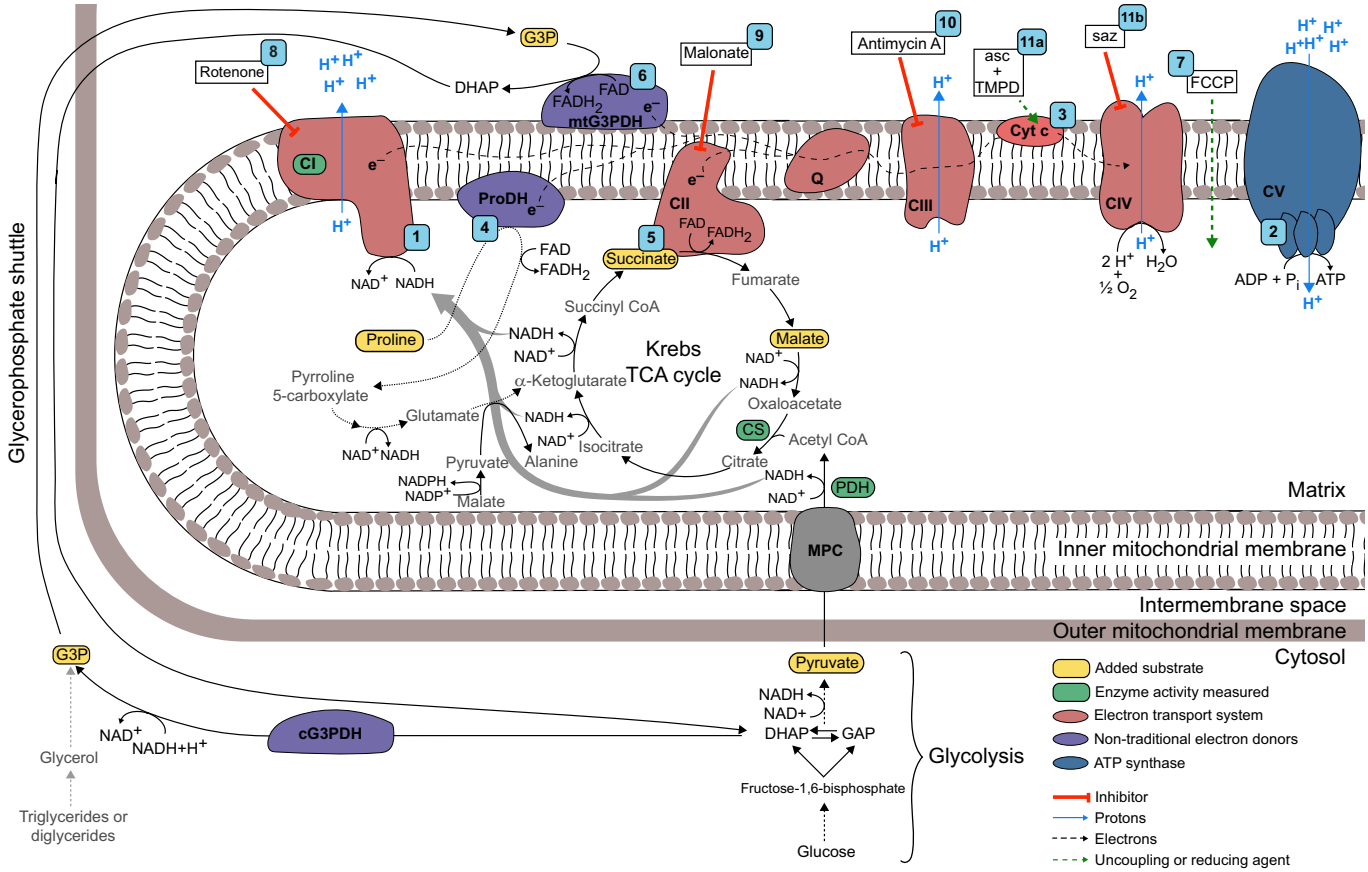

Fig. 1. Overview of mitochondrial metabolism and the substrate–uncoupler–inhibitor titration (SUIT) protocol used in the present study. Numbered blue squares refer to steps in the SUIT protocol (see Materials and Methods). In the cytosol, glycolysis transforms glucose into pyruvate, which is then transported to the mitochondrial matrix by the mitochondrial pyruvate carrier (MPC). In the matrix, pyruvate dehydrogenase (PDH) transforms pyruvate into acetyl coenzyme A (acetyl-CoA) and reduces NAD^+ to NADH. Acetyl-CoA, which can also be produced from fatty acid oxidation, enters the tricarboxylic acid (TCA) cycle where it participates in condensation with oxaloacetate to form citrate by citrate synthase (CS). The NADH reducing equivalents formed through the TCA cycle and PDH activity are used by complex I (CI) to transfer protons from the matrix to the intermembrane space. Succinate, a TCA cycle intermediate, is oxidized by complex II (CII) which transfers electrons to the ubiquinone (Q) pool via $FADH_2$. Proline, a non-traditional electron donor used by some insects, is fuelling proline dehydrogenase (ProDH), which transfers electrons directly to the Q pool but can also act as a carbon source and thus replenish the TCA cycle (anaplerotic function, dotted arrows). Glycerol-3-phosphate (G3P), derived from lipid catabolism or transformation of dihydroxyacetone phosphate (DHAP) from glycolysis, is shuttled into the intermembrane space where the mitochondrial glycerol-3-phosphate dehydrogenase (mtG3PDH) reduces the coenzyme FAD and donates electrons to the Q pool. Electrons from upstream complexes in the electron transport system (ETS) converge to the Q pool and subsequently go through complex III (CIII), where protons are pumped to the intermembrane space, and then via cytochrome c (Cyt c) to complex IV (CIV), where molecular oxygen is used as the final electron acceptor and protons are pumped to the intermembrane space. The proton gradient formed by the ETS is used by ATP synthase (complex V, CV) to form ATP through phosphorylation of ADP. For definitions, see List of abbreviations.

OXPHOS), FCCP (FCCP-ETS), malonate and antimycin A (ROX, subtracted from the other rates). This SUIT protocol took about 45 min until the final injection. The measurements described in this section were performed at Aarhus University, along with additional 'control' experiments using the full SUIT protocol described above (not shown). Chemicals were purchased from Millipore-Sigma (Oakville, ON, Canada or Søborg, Denmark).

Analysis of respiration data

All oxygen consumption rates are here reported as means±s.e.m. of mass-specific rates using the unit pmol O_2 s^{-1} mg^{-1} permeabilized thorax.

In some experiments, oxygen consumption rate did not stabilize following the addition of ADP (CI-LEAK to CI-OXPHOS transition) but stabilized with the addition of subsequent substrates in the protocol. We perceive these unstable preparations as a biological representation of a transition phenomenon rather than a technical error and in these cases, estimates of CI-OXPHOS oxygen consumption rates were also made during the unstable measurements (see Fig. S4). The unstable traces were observed in five species (not in *D. melanogaster*) and found scattered across temperatures 34, 38 and 42°C. Traces that displayed stable rates during CI-OXPHOS at 34, 38 and 42°C in the five species were analysed to find the average time required for the oxygen consumption rate to stabilize, and the overall mean (138±5 s) across temperatures and species was used to estimate the response to ADP in unstable traces (i.e. the oxygen consumption rate measured 133–143 s after the injection of ADP; see Fig. S4). The estimate of 'CI-OXPHOS' in preparations that did not show a stable oxygen consumption rate (OCR) following ADP injection is not directly comparable to the CI-OXPHOS reported from stable preparations, and accordingly the estimates were not used for calculation of the OXPHOS coupling efficiency ($j_{\approx P}$) and the substrate contribution ratio (SCR) of proline (see below).

Journal of Experimental Biology (2021) 224, jeb240960. doi:10.1242/jeb.240960

CI-LEAK and CI-OXPHOS were used to calculate the OXPHOS coupling efficiency ($j_{\approx P}$) at the level of CI:

$$j_{\approx P} = 1 - \frac{\text{CI-LEAK}}{\text{CI-OXPHOS}}. \quad (1)$$

A large increase in oxygen consumption following injection of ADP results in $j_{\approx P}$ approaching 1, which indicates a highly coupled system as electrons transported by CI are tightly coupled to oxidative phosphorylation, while an unaffected oxygen consumption rate ($j_{\approx P}$=0) indicates that oxidative phosphorylation does not exert flux control over the electrons transported from CI (Gnaiger, 2014).

The SCR, i.e. the relative contribution to increased oxygen consumption rate when adding a new substrate (proline, then succinate followed by G3P) was calculated as:

$$\text{SCR} = \frac{\text{OCR}_2 - \text{OCR}_1}{\text{OCR}_1}, \quad (2)$$

where OCR_1 is the oxygen consumption rate prior to injection of the new substrate (e.g. CI+ProDH-OXPHOS) and OCR_2 is the oxygen consumption rate with the new substrate injected (e.g. CI+ProDH+CII-OXPHOS). A value of SCR close to 0 indicates that the added substrate did not increase the oxygen consumption markedly, while SCR=1 indicates a 100% increase (doubling), SCR=2 indicates a 200% increase (tripling), and so forth. Note that the SCR does not contain information on how the change in oxygen consumption is distributed among different levels of the ETS (individual complexes and interactions between complexes), it is only a measure of the total change in oxygen consumption.

The maximal ETS capacity where electron transfer is not coupled to phosphorylation (FCCP-ETS) was compared with the maximal oxygen consumption rate coupled to phosphorylation (CI+ProDH+CII+mtG3PDH-OXPHOS) to calculate the non-coupled ratio, $ETS_{max}/OXPHOS_{max}$:

$$\text{ETS}_{\text{max}}/\text{OXPHOS}_{\text{max}} = \frac{\text{FCCP-ETS}}{\text{CI} + \text{ProDH} + \text{CII} + \text{mtG3PDH-OXPHOS}}. \quad (3)$$

If $ETS_{max}/OXPHOS_{max}$=1, then the ETS is already fully coupled to phosphorylation, while $ETS_{max}/OXPHOS_{max}$>1 indicates that the ETS is limited by the downstream process of phosphorylation, and thus has the capacity to increase electron transport when the limiting step is alleviated by adding the uncoupler FCCP.

Enzymatic activity

Measurement of enzymatic activity for all species was performed at similar temperatures to those for measurement of mitochondrial oxygen consumption [23.5, 30, 34, 38, 42 and 45°C; note the system could not be cooled to 19°C (replaced by 23.5°C) nor heated to 46°C (replaced by 45°C)]. For each species, 6 pools of female flies (4–7 days post-eclosion) were used (10 flies in each pool for all species except the large *D. immigrans* where only 5 flies were pooled), and all measurements were run with 2–3 technical replicates from each pool. Flies were chilled and their thoraces were dissected and stored at −80°C, until they were homogenized in phosphate-buffered saline (137 mmol l^{-1} NaCl, 2.7 mmol l^{-1} KCl, 10 mmol l^{-1} Na_2HPO_4, 1.8 mmol l^{-1} KH_2PO_4, pH 7.4) using a pellet pestle and the resulting homogenates were centrifuged at 750 ***g*** for 5 min at 4°C. The supernatant was then directly used for measurement of NADH:ubiquinone oxidoreductase (CI) and pyruvate dehydrogenase (PDH). The remaining supernatant was kept at −80°C for later measurement of citrate synthase (CS) and total protein content. All enzymatic activities were measured following protocols already established (Ekström et al., 2017; Cormier et al., 2019) using a BioTek Synergy H1 microplate reader (BioTek®, Montreal, QC, Canada). Enzymatic activity (EA) was calculated using the following equation:

$$\text{EA} = \frac{\Delta A \times V_{\text{f}} \times \text{DF}}{\varepsilon \times V_{\text{homo}} \times h}, \quad (4)$$

where ΔA represents the change in absorbance, V_f is the final volume in the well, DF represents the dilution factor, ε is the molar extinction coefficient, V_{homo} represents the volume of homogenate used and h is the height of the volume in the well (including the bottom thickness), calculated as $h=(4V)/(\pi d^2)$ where V is the final volume of the reaction (between 200 and 225 µl of reaction medium depending on the enzyme measured) and d is the diameter of the well. Concentrations for each compound of stock solutions used are described below.

CI (EC 7.1.1.2) activity was measured by following the reduction of 2,6-dichloroindophenol (DCPIP) at 600 nm (ε=19.1 ml cm^{-1} µmol^{-1}). Briefly, CI oxidizes NADH and the electrons produced reduce the ubiquinone 1 (UQ1) which subsequently delivers the electrons to DCPIP. After incubation of homogenates in a 100 mmol l^{-1} potassium phosphate buffer containing 0.5 mmol l^{-1} EDTA, 3 mg ml^{-1} BSA, 1 mmol l^{-1} $MgCl_2$, 2 mmol l^{-1} KCN, 4.2 µmol l^{-1} antimycin A, 75 µmol l^{-1} DCPIP and 65 µmol l^{-1} UQ1, pH 7.5, for 5 min in the plate reader at assay temperature, 0.14 mmol l^{-1} NADH was added to start the reaction, which was recorded for 10 min. The same reaction with 1 µmol l^{-1} rotenone was followed in parallel and the specific CI activity represented by the rotenone-sensitive activity was calculated.

PDH (EC 1.2.4.1) activity was measured using the reduction of *p*-iodonitrotetrazolium violet (INT) at 490 nm (ε=15.9 ml cm^{-1} µmol^{-1}) for 10 min after homogenates had been incubated in 50 mmol l^{-1} Tris-HCl, 0.1% (v/v) Triton-X 100, 1 mmol l^{-1} $MgCl_2$ and 1 mg ml^{-1} BSA complemented with 2.5 mmol l^{-1} NAD, 0.5 mmol l^{-1} EDTA, 0.1 mmol l^{-1} coenzyme A, 0.1 mmol l^{-1} oxalate, 0.6 mmol l^{-1} INT, 6 U ml^{-1} lipoamide dehydrogenase, 0.2 mmol l^{-1} thiamine pyrophosphate and initiated with 5 mmol l^{-1} pyruvate, pH 7.8.

CS (EC 4.1.3.7) activity was determined at 412 nm for 5 min by measuring the reduction of 5,5-dithiobis-2-nitrobenzoic acid (DTNB, ε=14.15 ml cm^{-1} µmol^{-1}; Riddles et al., 1979) using a 100 mmol l^{-1} imidazole-HCl buffer containing 0.1 mmol l^{-1} DTNB, 0.1 mmol l^{-1} acetyl coenzyme A (acetyl-CoA) and 0.15 mmol l^{-1} oxaloacetic acid, pH 8.0.

Total protein content was measured using the bicinchoninic acid method (Smith et al., 1985) and enzymatic activity is reported as U g^{-1} protein, where U represents 1 µmol of substrate transformed to product in 1 min.

Statistics

Statistical data analyses were performed in *R* version 3.6.2 (http://www.R-project.org/).

For comparison of oxygen consumption rates, calculated ratios and enzymatic activity, statistical analyses were performed across temperatures within substrate combinations (or ratio type or enzyme) within species using one-way ANOVA and Tukey's *post hoc* test using the *emmeans*-function (estimated marginal means) in the emmeans-package in *R* (https://github.com/rvlenth/emmeans).

Oxygen consumption rates from stable and unstable traces (deemed after ADP injection) were compared using Welch two-sample *t*-tests (see Fig. S4).

Journal of Experimental Biology (2021) 224, jeb240960. doi:10.1242/jeb.240960

To examine the relationship between mitochondrial function and species heat tolerance, (stable) CI-OXPHOS and CI+ProDH+CII+mtG3PDH-OXPHOS rates measured at 30–46°C were normalized to the mean of said rate at 30°C. In the two-temperature interval where a 50% reduction in rate occurred, a linear regression was used to estimate the temperature where the OCR was 50% of the value at 30°C, and this temperature was then regressed against the species temperature tolerance expressed as the temperature resulting in knockdown after 1 h (see 'Experimental animals' above).

RESULTS

High temperature results in loss of mitochondrial CI oxidative capacity, but maximal respiration is partially rescued by oxidation of alternative substrates

To examine the sensitivity of mitochondrial function to high temperature, mass-specific OCR was measured at six temperatures (19, 30, 34, 38, 42 and 46°C) in permeabilized thoraces from six *Drosophila* species over multiple steps of the ETS. For each step, OCRs were evaluated between assay temperatures within species

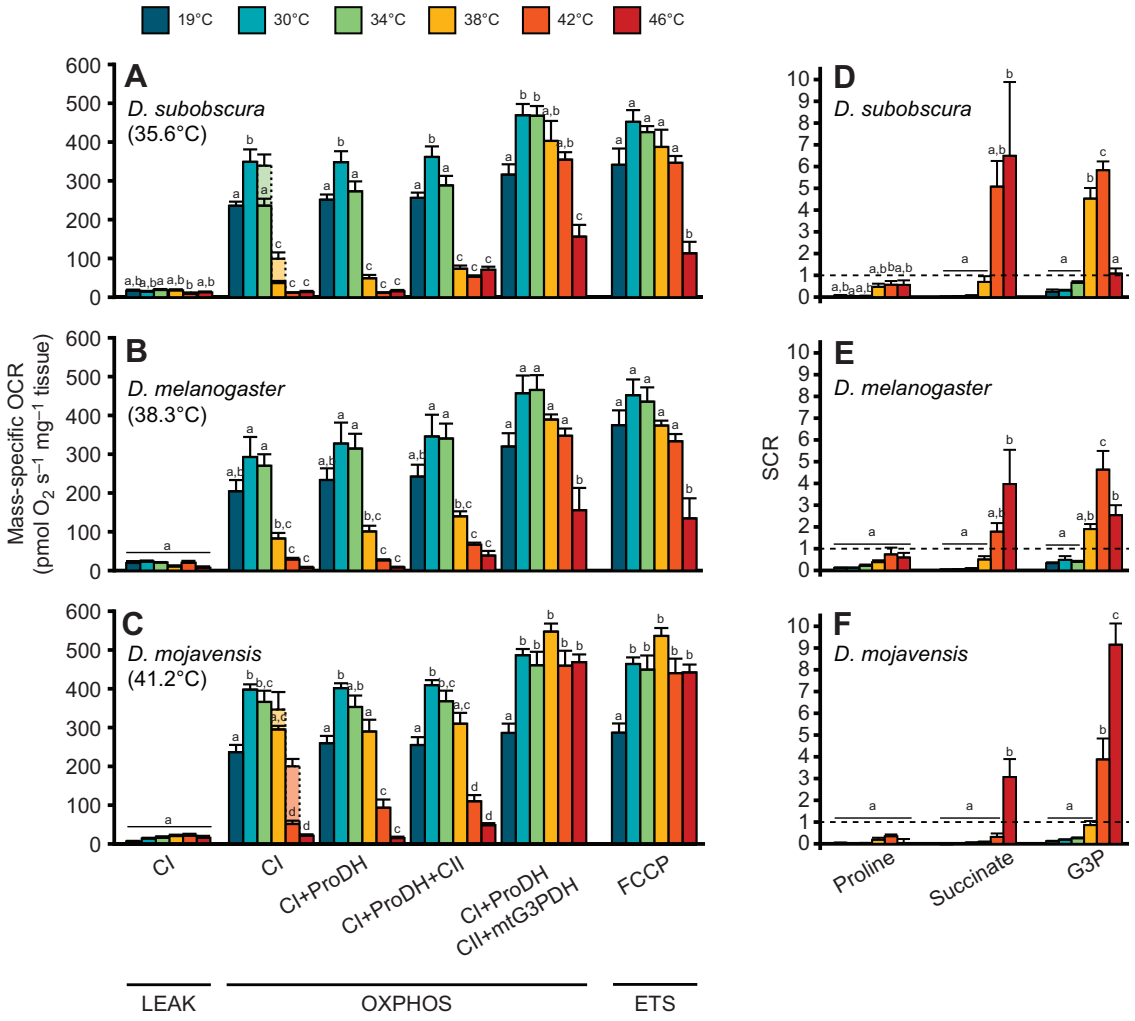

Fig. 2. Mass-specific oxygen consumption rate (OCR) in permeabilized *Drosophila* thoraces and calculated substrate contribution ratios for three of the tested species. (A–C) Using a SUIT protocol (Fig. 1; see Materials and Methods), OCR was measured in the LEAK (without ADP), OXPHOS (oxidative phosphorylation, respiration coupled to phosphorylation with saturating ADP) and ETS (electron transport system, non-coupled from phosphorylation) states. The SUIT protocol was performed at six assay temperatures, 19°C (maintenance temperature, dark blue) and 30, 34, 38, 42 and 46°C, covering benign and stressfully high temperatures for the *Drosophila* species tested: *D. subobscura* (A), *D. melanogaster* (B) and *D. mojavensis* (C) in increasing order of heat tolerance (the temperature estimated to cause knockdown after 1 h is given in parentheses; Jørgensen et al., 2019). OCRs are reported as means±s.e.m.; sample size for each species×temperature combination is described in Table 1. In some preparations, oxygen flux did not stabilize following the injection of ADP (CI-OXPHOS) and instead an estimate of the flux was made (lighter shaded, dashed lined bars, see Materials and Methods and Fig. S4). Within each step of the protocol (cluster of bars), the OCRs were compared between temperatures within species using a one-way ANOVA with a Tukey's *post hoc* test, and dissimilar letters within a cluster indicate statistically significant differences ($P<0.05$). (D–F) Substrate contribution ratio (SCR) for the three sequentially injected substrates: proline, succinate and G3P. SCR was calculated as the ratio between the increase in OCR following injection of the new substrate compared with the prior OCR, and as such the SCR of proline is based on the change compared with CI-OXPHOS, SCR of succinate on CI+ProDH-OXPHOS and SCR of G3P on CI+ProDH+CII-OXPHOS. The scale of the SCRs refers to fold-changes from the base rate, i.e. 0 means that the added substrate did not change the OCR, 1 refers to a doubling (100% increase from base rate), 2 to a 3-fold change (200%), etc. SCRs are reported as means±s.e.m.; sample size for each species×temperature combination is described in Table 1. For preparations that were unstable at CI-OXPHOS, it was not possible to calculate the SCR for proline, and accordingly values of SCR for proline are based solely on stable CI-OXPHOS preparations, while SCR for succinate and G3P were calculated for all preparations. Within each species, SCRs were compared between temperatures using a one-way ANOVA with a Tukey's *post hoc* test, and dissimilar letters within a cluster indicate significant differences ($P<0.05$). In *D. melanogaster*, a significant effect of temperature was found for proline ($F_{5,37}=2.571$, $P=0.043$), but the *post hoc* test failed to reveal significant contrasts between temperatures. The results from the other three species are presented in Fig. S1.

Journal of Experimental Biology (2021) 224, jeb240960. doi:10.1242/jeb.240960

with temperature as the fixed factorial variable using one-way ANOVA and, when applicable, pairwise comparisons with Tukey adjustment of *P*-values (*F*-values; Table S1). To simplify the graphical presentation of the results, three species (*D. immigrans*, *D. mercatorum* and *D. virilis*) are shown in Figs S1 and S2, and thus only measurements from *D. subobscura*, *D. melanogaster* and *D. mojavensis* are presented graphically below. The omitted species have an organismal heat tolerance that approximately corresponds to that of the presented species in the order above [e.g. *D. immigrans* and *D. subobscura* have similar (low) heat tolerance].

LEAK-state respiration was assessed at the level of complex I (CI-LEAK) by injecting pyruvate and malate, and this corresponds to the oxygen consumption required to offset the proton leak across the inner mitochondrial membrane from the intermembrane space without phosphorylation. CI-LEAK was generally low in all species across temperatures. However, assay temperature was found to affect the rate in *D. immigrans* (Fig. S1A), *D. subobscura* (Fig. 2A), *D. mercatorum* (Fig. S1B) and *D. melanogaster* (Fig. 2B), though in *D. melanogaster* the *post hoc* test failed to separate the temperatures. No statistically significant effects of assay temperature were found in *D. virilis* (Fig. S1C) or *D. mojavensis* (Fig. 2C).

Next, CI respiration was measured by injecting ADP to couple electron transport (and hence oxygen consumption) to phosphorylation (CI-OXPHOS). Assay temperature was found to affect CI-OXPHOS in all six species (one-way ANOVA, $P<0.001$), and there was a general pattern of how this temperature effect was manifested. Increasing temperature from the acclimation temperature (19°C) to 30°C increased CI-OXPHOS for all species (Fig. 2A–C; Fig. S1A–C), although for *D. immigrans* and *D. melanogaster* this increase was not statistically significant (Tukey's *post hoc* adjustment: $P=0.177$ and $P=0.281$, respectively). In measurements performed at 34, 38 and 42°C, we observed several unstable preparations with distinctive features; a sharp increase in OCR after ADP injection, which was quickly followed by a gradual, consistent decrease that persisted until subsequent substrate injections, which led to stabilization of the OCR (see Fig. S4). The analysis and quantification of these unstable traces is discussed in the paragraph below. At 34°C, stable CI-OXPHOS rates were similar to those measured at 30°C (*D. immigrans*, *D. melanogaster*, *D. virilis* and *D. mojavensis*), while CI-OXPHOS rate decreased in *D. subobscura* and *D. mercatorum*, albeit not significantly in the latter species. At 38°C, CI-OXPHOS decreased significantly compared with that at 34°C in the four least heat

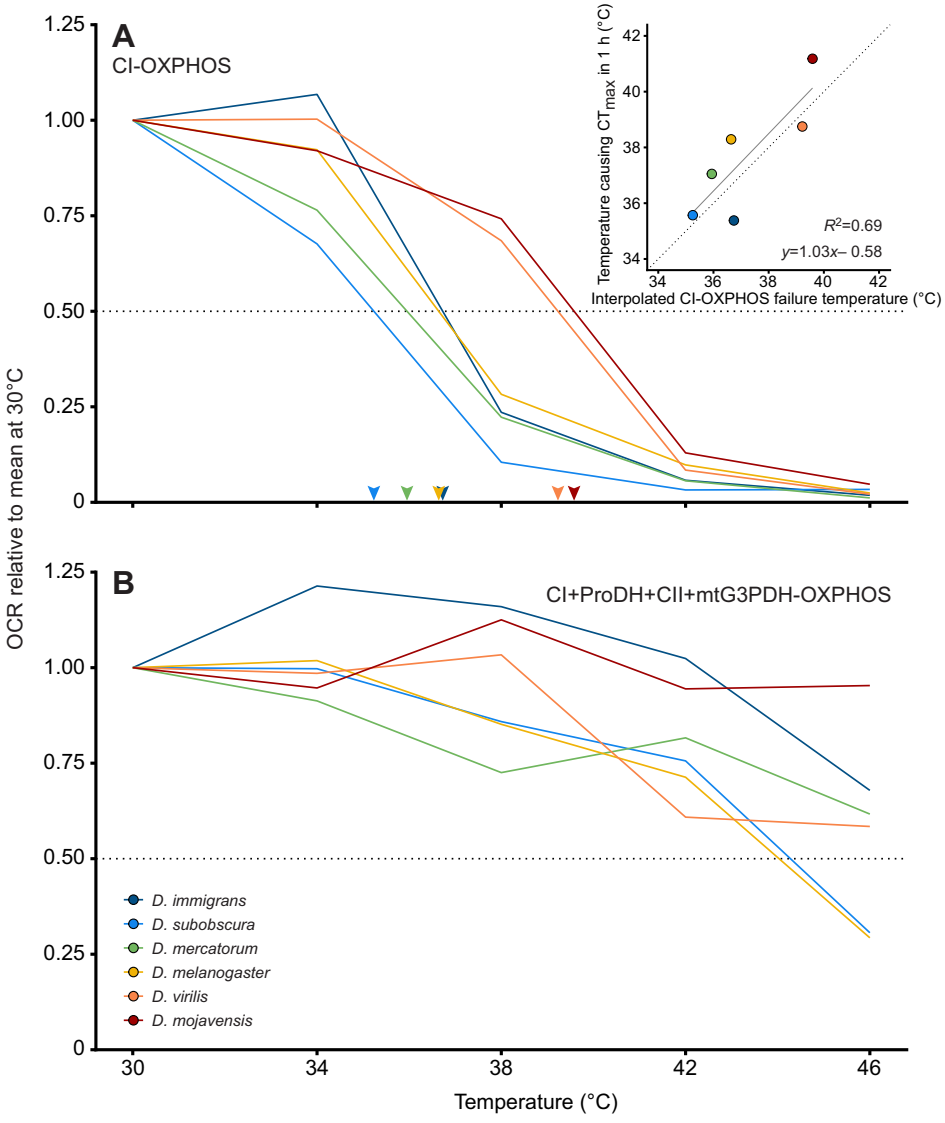

Fig. 3. OCR relative to mean rate measured at 30°C. Species lines (see key) connect the calculated relative rates at the five assay temperatures (from Fig. 2; Fig. S1) for (A) CI-OXPHOS and (B) CI+ProDH+CII+ mtG3PDH-OXPHOS. The dotted line indicate 50% of the rate measured at 30°C and coloured arrowheads in A indicate the temperature where CI-OXPHOS was reduced by 50% (by interpolating between rates at the two assay temperatures that frame the 50% reduction, e.g. 34 and 38°C). Inset: interpolated estimates of CI-OXPHOS failure temperature plotted against the temperature resulting in knockdown (CT_{max}) in 1 h (from Jørgensen et al., 2019) along with a linear regression (solid line) and the line of unity (dotted line).

Journal of Experimental Biology (2021) 224, jeb240960. doi:10.1242/jeb.240960

Table 1. OXPHOS coupling efficiency ($j_{\approx p}$) for each *Drosophila* species at each temperature

Temperature (°C)	*D. immigrans*	*D. subobscura*	*D. mercatorum*	*D. melanogaster*	*D. virilis*	*D. mojavensis*
19	0.92±0.01 (8/8)^{A}	0.93±0.01 (7/7)^{A}	0.98±0.00 (8/8)^{A}	0.90±0.02 (7/7)^{A}	0.95±0.01 (7/7)^{A}	0.97±0.01 (7/7)^{A}
30	0.95±0.01 (7/7)^{A}	0.96±0.00 (7/7)^{A}	0.97±0.00 (7/7)^{A}	0.89±0.03 (8/8)^{A}	0.96±0.01 (7/7)^{A}	0.97±0.01 (7/7)^{A}
34	0.94±0.01 (7/10)^{A}	0.95±0.01 (2/8)^{A}	0.92±0.01 (5/8)^{A}	0.92±0.01 (7/7)^{A}	0.97±0.01 (7/7)^{A}	0.96±0.01 (7/7)^{A}
38	**0.78±0.04** (5/9)^{A}	**0.38±0.10** (3/8)^{B}	0.98±NA (1/7)^{A}	0.87±0.03 (7/7)^{A}	0.94±0.01 (3/7)^{A}	0.90±0.00 (3/8)^{A,B}
42	**0.20±0.07** (7/7)^{B}	**0.27±0.07** (8/8)^{B,C}	**0.38±0.07** (7/7)^{B}	**0.25±0.12** (8/8)^{B}	**0.43±0.14** (6/7)^{B}	**0.38±0.20** (2/7)^{B,C}
46	**0.01±0.18** (7/7)^{B}	**0.04±0.07** (6/6)^{C}	**0.23±0.07** (7/7)^{B}	**0.06±0.20** (6/6)^{B}	**0.27±0.10** (7/7)^{B}	**0.32±0.15** (6/6)^{C}

Data are means±s.e.m. Note for *D. mercatorum* at 38°C, s.e.m. could not be calculated (NA), as it was only possible to calculate $j_{\approx p}$ for a single preparation. Values of $j_{\approx p}$ close to 1 indicate well-coupled mitochondria while values close to 0 indicate poorly coupled mitochondria, at least at the level of complex I. As it was not possible to measure the parameters required for calculation of $j_{\approx p}$ in unstable preparations, the mean and s.e.m. are based solely on stable preparations (the first number in the parentheses; the second number refers to the total number of preparations measured for each species×temperature combination). Within a species, dissimilar letters indicate statistically significant differences in the OXPHOS coupling efficiency between temperatures (one-way ANOVA with Tukey's *post hoc* test, $P<0.05$). Values of s.e.m.<0.005 are reported as 0.00 to reduce decimal places. Oxygen coupling efficiency values in bold are those that drop below the 'healthy' value 0.8 (linearized transformation of respiratory control ratio, RCR, of 5; Gnaiger, 2014).

tolerant species, i.e. *D. immigrans*, *D. subobscura*, *D. mercatorum* and *D. melanogaster* (Fig. 2A,B; Fig. S1A,B). The heat tolerant *D. virilis* and *D. mojavensis* also showed a trend for decreased CI-OXPHOS at 38°C, but the rates were not significantly different from those measured at 34°C (Fig. 2C; Fig. S1C). At temperatures above 38°C, all species showed significantly decreased CI-OXPHOS, with non-significant differences between rates measured at 42 and 46°C, although the mean rates were almost always lower at 46°C. Accordingly, all species had CI-OXPHOS rates at the highest temperatures that were significantly lower than at their acclimation temperature (19°C). For each species, CI-OXPHOS rate at 30–46°C was normalized to the mean rate at 30°C, and an estimate of the temperature where OCR was reduced to 50% was regressed against a measure of species heat tolerance (Fig. 3A). This regression yielded a positive correlation (R^2=0.69) that was not significantly different from the line of unity (P=0.938).

As stated above, unstable CI-OXPHOS measurements were found in five of the six species (not *D. melanogaster*), and were distributed such that *D. immigrans*, *D. subobscura* and *D. mercatorum* (heat sensitive) displayed instability at 34 and 38°C, while unstable CI-OXPHOS traces were found at 38 and 42°C in *D. virilis* and *D. mojavensis* (heat tolerant) (Table 1). We believe that this unstable measurement represents a biological transition from high to low levels of CI-OXPHOS, and to quantify this observation, we obtained the OCR following ADP injection at the time where 'stable' traces would have stabilized CI-OXPHOS (138±5 s) to generate a proxy for CI-OXPHOS in the unstable preparations. The mean of these 'unstable' rates was generally higher than the mean of stable CI-OXPHOS at the same temperature within a species (compare lightly and fully shaded bars in Fig. 2; Figs S1 and S4), which indicates that the unstable, declining traces represent a transition state prior to lower and potentially stable rates (see Discussion).

Following measurement of CI-OXPHOS, cytochrome *c* was injected to test the condition of the outer mitochondrial membrane, and a reduced response (<15% increase in OCR) was taken as an indication that the outer mitochondrial membrane was intact following permeabilization. Then proline (CI+ProDH-OXPHOS) and succinate (CI+ProDH+CII-OXPHOS) were injected, and the general patterns for the thermal sensitivity of the resulting OCRs were similar to the patterns observed for CI-OXPHOS (similar lettering within species in Fig. 2A–C; Fig. S1A–C), except that these traces were all stable, regardless of the stability immediately following ADP injection (CI-OXPHOS).

Injection of G3P gave rise to the maximal OCR during the OXPHOS state, allowing us to evaluate the convergent electron flow into the ETS in a coupled state. The OCRs measured as CI+ProDH+CII+mtG3PDH-OXPHOS may be driven by different (unknown) contributions of mitochondrial complexes and dehydrogenases, and it is therefore of interest to examine the rates both as a measure of maximal coupled respiratory capacity and to indicate the relative contribution of each substrate to increase OCR. The latter will be examined in the section on substrate switching, below.

Maximal oxygen consumption rate in the coupled state (CI+ProDH+CII+mtG3PDH-OXPHOS) increased from 19°C to 30–38°C, with slight, non-significant decreases between 34 and 38°C in all species except the heat-tolerant *D. virilis* and *D. mojavensis* (Fig. 2A–C; Fig. S1A–C). At 42°C, the maximal rates were mostly higher than those measured at 19°C (however, only significantly in *D. mojavensis*; Fig. 2C), but lower than at 38°C (though only significantly in *D. virilis*). At the most extreme temperature, 46°C, OCRs in *D. immigrans*, *D. mercatorum* and *D. virilis* were lower compared with those for the other 'high' temperatures (everything above 19°C), but similar to the rates measured at 19°C (Fig. S1A–C), while in *D. subobscura* and *D. melanogaster*, the rates at 46°C were significantly lower than at all other temperatures (Fig. 2A,B). The most heat tolerant species, *D. mojavensis*, displayed a different response to the extreme temperature and maintained a high maximal OCR, which was similar to that at the other 'high' temperatures (>19°C) and significantly higher than the rate measured at 19°C (Fig. 2C). Hence, all species were able to maintain high maximal respiration rates at species-specific temperatures that are incompatible with survival for more than a few minutes (Fig. 3B).

After the maximal coupled respiration rate had been measured, FCCP was added to measure OCR in the non-coupled state, as this uncoupler allows protons to cross the inner mitochondrial membrane and thus alleviates any limitations to respiration by phosphorylation. The non-coupled respiration rates (FCCP-ETS) are presented in Fig. 2A–C and Fig. S1A–C, but another way to examine the potential constraints of the phosphorylating system on the ETS capacity is to calculate the non-coupled ratio ($ETS_{max}/OXPHOS_{max}$) by dividing the non-coupled rate by the maximal coupled rate (FCCP-ETS/CI+ProDH+CII+mtG3PDH-OXPHOS; Table S2). In all six species, the highest values of $ETS_{max}/OXPHOS_{max}$ were observed at the lower range of temperatures but were very close to 1.0. This suggests that the processing of protons by the ATP synthase to phosphorylate ADP to ATP was not limiting the transport of electrons by the ETS and that the mixture of substrates used allowed the ETS to reach its full capacity. The $ETS_{max}/OXPHOS_{max}$ values decreased slightly with temperature between 19 and 42°C but remained close to the

lowest theoretical value of 1.0. At 46°C, more marked decreases of $ETS_{max}/OXPHOS_{max}$ were observed (such as in *D. subobscura*; Table S2), which could indicate a damaged ETS or increased permeability of the inner mitochondrial membrane due to temperature (not examined in the present study).

Maximal activity of CIV, the last respiratory enzyme of the ETS where oxygen is used as the final electron acceptor, was measured after inhibition of complexes I, II and III and was stimulated by the artificial substrate TMPD (along with ascorbate; Fig. S5). When temperature was increased from 19 to 30°C, all species showed increased CIV activity, which for *D. subobscura*, *D. mercatorum*, *D. virilis* and *D. mojavensis* was significantly higher ($P \leq 0.003$, one-way ANOVA with Tukey's *post hoc* adjustment), but did not reach the level of significance in *D. immigrans* and *D. melanogaster* ($P=0.121$ and 0.696, respectively). At 34°C, CIV activity was mostly similar or not significantly increased compared with that at 30°C ($P \geq 0.081$), and likewise when CIV activity measured at 38°C was compared with that at 34°C. However, *D. immigrans* showed a significant increase in CIV activity ($P=0.003$), and also reached its maximal capacity at this temperature (38°C). *Drosophila mercatorum* and *D. melanogaster* also peaked in measured CIV capacity at 38°C, while *D. subobscura* and *D. virilis* showed a plateau-like CIV capacity from 30 to 38°C, with slightly higher capacity at the lower temperatures. The CIV capacity of the most heat tolerant species, *D. mojavensis*, peaked at 42°C. This was, however, not statistically different from the activity observed at 38°C ($P=0.993$). For the other species, 42°C decreased CIV capacity, although only significantly in *D. immigrans* and *D. mercatorum* ($P<0.001$ and $P=0.007$, respectively). At the extreme temperature of 46°C, all species showed significantly reduced rates compared with those at the other 'high' temperatures, while CIV activity was mostly similar to the rate measured at 19°C (only *D. subobscura* showed a significantly lower rate than at 19°C).

High temperature diminishes mitochondrial coupling at the level of CI

The OXPHOS coupling efficiency ($j_{\approx p}$, unitless) at the level of CI was calculated as 1−(CI-LEAK/CI-OXPHOS), a linearized form of the traditional respiratory control ratio (RCR) which describes the flux control of ADP on CI-supported respiration (Table 1). Here, $j_{\approx p}$ approaching 1 indicates a maximally coupled CI and $j_{\approx p}=0$ indicates a non-ADP controlled CI respiration. All species showed high values of $j_{\approx p}$ at 19, 30 and 34°C (range: 0.892–0.972), above the 0.8 value that is traditionally expected from 'healthy', functional mitochondria (RCR of 5 transformed to $j_{\approx p}$; Gnaiger, 2014), and within species these values were not significantly different ($P \geq 0.949$, one-way ANOVA with Tukey's *post hoc* adjustment). At 38°C, *D. subobscura* displayed a reduced $j_{\approx p}$ (0.384±0.104) compared with that at the lower temperatures ($P<0.003$), and similar reductions were found at 42°C for *D. immigrans* (0.195±0.069, $P<0.001$), *D. mercatorum* (0.381±0.072, $P<0.001$), *D. melanogaster* (0.252±0.123, $P<0.001$) and *D. virilis* (0.431±0.136, $P<0.006$). For *D. mojavensis*, $j_{\approx p}$ at 42°C was reduced compared with that at 19–34°C (0.377±0.201, $P<0.009$), but the value was not significantly different from that at 38°C ($P=0.058$). However, at the most extreme temperature, 46°C, all species displayed highly reduced values of $j_{\approx p}$ compared with those at the lower temperatures (Table 1).

Temperature-dependent shift in mitochondrial substrate oxidation

Using the sequential injection of substrates in the SUIT protocol allowed us to calculate the relative contribution to the OCR for each substrate (i.e. the SCR; Fig. 2D–F; Fig. S1D–F). At the lower temperatures (19–34°C), it is clear from the SCRs of all species that addition of the three substrates proline, succinate and G3P did not stimulate the OCR markedly above that measured with only pyruvate and malate. This is in marked contrast to the situation at higher temperatures, where SCRs were elevated for proline and succinate, particularly at 42 and 46°C, and SCRs for G3P were very high at 38–46°C. Across species, the relative effect of adding proline was smaller than the effect of adding succinate or G3P. Only in *D. subobscura* and *D. mercatorum* was it possible to detect a temperature effect on the stimulation from proline injection and distinguish between temperatures (with larger responses at higher temperatures) (Fig. 2D; Fig. S1E). Succinate gave high values of SCR in *D. immigrans* and *D. subobscura* and intermediate values in *D. melanogaster* at both 42 and 46°C, while large effects of succinate were only found at 46°C in *D. mercatorum*, *D. virilis* and *D. mojavensis*. For G3P, *D. immigrans* (Fig. S1D) and *D. subobscura* (Fig. 2D) showed significant increases in SCR at 38°C, while this effect was only significant at 42°C for the remaining four species (Fig. 2B,C; Fig. S1B,C). At 46°C, SCR for G3P decreased in most species except *D. virilis* and *D. mojavensis*, in which SCR increased (though only significantly in *D. mojavensis*; Fig. 2C).

The high SCR values indicate that the OCR was markedly stimulated by injection of these substrates. In other words, when CI fails (see above), other substrates can take over to support respiration. An additional set of experiments was performed to examine whether the increased effect of injection of alternative substrates (proline, succinate and G3P) at high temperatures was attributable to the removal of a CI 'masking effect' through the temperature-induced breakdown of CI-OXPHOS, or instead that the utilization processes of alternative substrates were temperature dependent. Specifically, a second SUIT protocol was designed to investigate whether proline and G3P could facilitate high OCRs at 34°C, a temperature where CI-OXPHOS is high (using the standard SUIT protocol; Fig. 2A–C), when their effect on OCR is marginal using the standard protocol at this temperature. The OCRs measured with the two SUIT protocols are not directly comparable, but when we tested *D. subobscura*, *D. melanogaster* and *D. mojavensis*, we found that proline and particularly G3P could sustain high OCRs at 34°C, when CI was artificially inhibited with rotenone prior to substrate injection (Fig. S3). We also inhibited CI at 42°C, a temperature at which CI was markedly depressed when measured using the standard protocol (Fig. 2A–C), and saw a similar large contribution of particularly G3P to oxygen consumption (Fig. S3).

Breakdown of CI-mediated respiration is not related to a loss of CI enzyme activity

To examine whether the breakdown of CI-OXPHOS observed at the higher assay temperatures was related to temperature-induced disruption of enzymatic function in the electron transporting enzyme itself, enzymatic catalytic capacity was measured at a range of temperatures (23.5–45°C). CI showed stable increases in enzymatic catalytic capacity with temperature in all species (Fig. 4A; Fig. S2A), with no apparent breakdown in contrast to the high-resolution respirometry experiments. Next, we measured PDH, which oxidizes pyruvate into acetyl-CoA and thus links glycolysis with the tricarboxylic acid (TCA) cycle while producing NADH that will feed electrons to CI (Fig. 1). For all species, the enzymatic activity of PDH increased with temperature, until conversion rates dropped in species with low to moderate heat tolerance at 42–45°C (*D. immigrans*, *D. subobscura*,

Journal of Experimental Biology (2021) 224, jeb240960. doi:10.1242/jeb.240960

D. melanogaster and *D. mercatorum*), although not significantly in *D. mercatorum* (Fig. 4B; Fig. S2B). In the heat tolerant species (*D. virilis* and *D. mojavensis*), PDH activity increased or remained the same (as at 42°C) at 45°C. PDH thus showed species-specific responses to increased temperature that may relate to species heat tolerance. Finally, we measured the activity of CS, which facilitates the condensation of acetyl-CoA with oxaloacetate to form citrate in the TCA cycle (Fig. 1). CS showed a similar reaction to high temperature in all species (Fig. 4C; Fig. S2C), with activity increasing from 23.5 to 30°C. Conversion rates levelled at 34°C (with small increases in *D. immigrans* and *D. melanogaster*), then dropped significantly at 38°C (*D. immigrans*, *D. mercatorum* and *D. mojavensis*) and 42°C in *D. subobscura*, *D. melanogaster* and *D. virilis*. Accordingly, CS displayed heat-induced perturbation of enzymatic catalytic capacity in all six species; however, the pattern did not follow species heat tolerance to the same degree as observed for PDH activity.

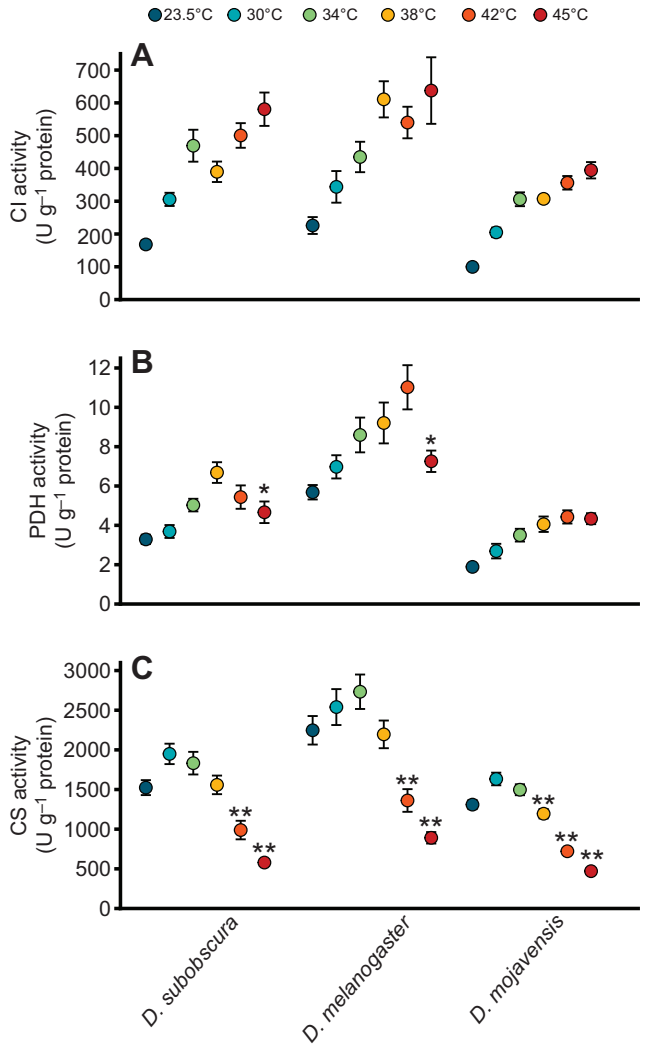

Fig. 4. Mitochondrial enzymes display divergent responses to high temperature. Enzymatic activity (EA) was measured in homogenized thoraces for (A) NADH:ubiquinone oxidoreductase (CI), (B) PDH and (C) CS, here shown for three species (see Fig. S2 for the other species). Enzymatic activity is reported as means±s.e.m. (U represents 1 μmol substrate transformed to product in 1 min). Notice that the temperatures used for measurements are not the same as those used for high-resolution respirometry (23.5 and 45°C replace 19 and 46°C, respectively; see Materials and Methods). Asterisks denote statistically significant differences between the measurements at higher temperatures than the temperature where the maximal enzymatic catalytic capacity was observed; **P*<0.05 and ***P*<0.001, one-way ANOVA with Tukey *post hoc* adjustments.

DISCUSSION

In the present study, we measured mitochondrial respiration rates in six *Drosophila* species with differing heat tolerance at temperatures ranging from benign to around and above species tolerance limits. With this design, we examined how temperature affects mitochondrial function, and whether loss of mitochondrial function can be related to organismal heat tolerance.

Mitochondrial function persists at temperatures above species heat tolerance

Several studies on ectotherms suggest that mitochondria are more heat tolerant than the animal as a whole (Chung and Schulte, 2020), and in insects a mitochondrial 'hyperthermic overdrive' in which mitochondria perform rapid aerobic metabolism is observed after the loss of higher organismal function (Heinrich et al., 2017; Mölich et al., 2013). In accordance, a recent study on the honey bee *Apis mellifera* found that mitochondrial respiration was intact at 50°C (Syromyatnikov et al., 2019), which is higher than or equal to the CT_{max} measured in two subspecies of *A. mellifera* using thermolimit respirometry (Kovac et al., 2014). In the *Drosophila* system, we found similar evidence for sustained mitochondrial function at high temperatures as all species were able to maintain high oxygen consumption rates at temperatures above their organismal heat limit (as characterized in Jørgensen et al., 2019; Fig. 3B). However, our results show that this mitochondrial heat tolerance is highly dependent on the oxidative substrates used to fuel respiration.

Hyperthermic breakdown of CI-supported respiration

Energetic demand increases with temperature in ectotherms, and accordingly the oxygen consumption related to mitochondrial aerobic ATP production often follows. When temperature was increased from the acclimation temperature (19°C) to 30°C, a high yet benign temperature for all of the species, we observed a general increase in maximal oxygen consumption rate under OXPHOS conditions (CI+ProDH+CII+mtG3PDH-OXPHOS), which was primarily driven by increased CI-supported oxygen consumption (Fig. 2A–C; Fig. S1A–C). The OCRs measured in *D. melanogaster* for each step of the SUIT protocol at 19 and 30°C were similar to previous measurements using the same protocol at 24°C in that species (Cormier et al., 2019). At 34°C, however, maximal oxygen consumption stagnated, and in some preparations of the three least heat tolerant species (*D. immigrans*, *D. subobscura* and *D. mercatorum*), the OCR did not stabilize following ADP injection (CI-OXPHOS; Fig. 2; see Figs S1 and S4), which was again observed at 38°C in the same species. Likewise, at 38°C, some of the preparations from the heat tolerant species *D. virilis* and *D. mojavensis* displayed this inability to maintain a stable CI-OXPHOS, and for these species the phenomenon persisted at 42°C (Fig. 2; Figs S1 and S4). It was only in *D. melanogaster*, a moderately heat tolerant species for which this SUIT protocol was optimized, that we did not observe this. Instead, this species was characterized by an abrupt decrease in CI-OXPHOS when temperature was increased from 34 to 38°C (Figs 2B and 3A) which was also observed in the stable CI-OXPHOS traces in the other species (at 34–38°C or 38–42°C depending on the species). Given the stabilization of OCR that occurred in all preparations with unstable CI-OXPHOS following injection of subsequent substrates, we suggest that the unstable traces represent a transition state between high ('normal') CI-OXPHOS and reduced CI-

OXPHOS, and, furthermore, from the temperature interval where it is observed and its prevalence that this is not a random phenomenon. These findings indicate a hyperthermic breakdown of CI-supported respiration. Indeed, it has been shown that NADH-dependent (i.e. CI-supported) OCR measured in *in vivo* heat-treated blowflies was reduced by 50% compared with that in non-heated controls (El-Wadawi and Bowler, 1996). CI has also been suggested to be a primary site of heat failure in liver mitochondria from marine fishes (Chung et al., 2018; Martinez et al., 2016), in marine crustaceans (Iftikar et al., 2010), as well as in maize (Pobezhimova et al., 1996). In the present study, the OXPHOS coupling efficiency $j_{\approx P}$ at the level of CI (the linearized form of the RCR) decreased with higher temperature (Table 1), which is an obvious consequence of the hyperthermic decrease in CI-OXPHOS rather than an increase in CI-LEAK, as previously observed (Hilton et al., 2010; Iftikar et al., 2010, 2014; Lemieux et al., 2010b). Accordingly, indications of a hyperthermic breakdown of CI respiration calls for examination of the underlying cause(s) but also of how mitochondria maintain function under this impairment, considering the observed ability to maintain persistently high maximal OCRs across a wide range of high temperatures.

CI, or NADH:ubiquinone oxidoreductase, is the major entry point for electrons into the ETS (in the inner mitochondrial membrane; Fig. 1) via oxidation of mitochondrial NADH produced by metabolic pathways such as the TCA cycle, pyruvate oxidation and β-oxidation of fatty acids (Hirst, 2010). As mitochondrial membranes are impermeable to NADH and NAD^+, CI is also an important regulator of the matrix redox pool (NAD^+/NADH ratio), which is required for the TCA cycle and various enzyme functions to continue (Sacktor, 1975). As CI-OXPHOS decreased at high temperatures in all of the species tested, we measured the enzymatic activity of CI to examine whether this decline was due to impaired enzyme function. We found that, at least in homogenized thoraces, CI activity did not suffer from a hyperthermic breakdown. Instead, enzymatic catalytic capacity increased with temperature, and peaked at 45°C (the highest temperature tested) (Fig. 4A; Fig. S2A). Thus, it is likely that the limitation of CI-OXPHOS observed here at high temperature occurs upstream of CI. A previous study in tobacco hornworm (*Manduca sexta*) reported that the substrate oxidation system governs a significant portion of the temperature effect on maximal mitochondrial respiration (Chamberlin, 2004). The PDH complex is a potential candidate explaining the observed decrease in CI-OXPHOS (Blier et al., 2014; Lemieux et al., 2010a) (Fig. 1). PDH activity increased with temperature, but above 38°C, there were species-specific differences in the reaction patterns (Fig. 4B; Fig. S2B). In the least heat tolerant species (*D. immigrans* and *D. subobscura*), activity decreased at 42 and 45°C, while in the moderately heat tolerant species (*D. mercatorum* and *D. melanogaster*), it increased up to 42°C and then decreased at 45°C. Finally, in the most heat tolerant species, *D. virilis* and *D. mojavensis*, PDH activity increased continuously or stagnated at 45°C. These interspecific patterns could be related to species heat tolerance, as observed for other enzymes (Dahlhoff and Somero, 1993; Hochachka and Somero, 2002). However, the temperatures at which declines in PDH activity were observed are higher than the temperature interval (34–42°C) where CI-OXPHOS rates were found to decrease, and notably for *D. virilis and D. mojavensis*, in which PDH activity did not appear to be compromised at all. Lastly, we also measured the activity of CS (Fig. 1). Generally, CS activity increased from 19 to 30°C but decreased slightly in most species at 34°C before it progressively dropped as temperature was raised to 45°C (Fig. 4C; Fig. S2C). Unlike for PDH activity, there was no clear pattern for the decrease in enzymatic activity between species that could potentially be related to their heat tolerance. Instead, it seems that CS is generally challenged at high temperatures in *Drosophila*. Heart CS (and PDH) activity was found to decrease at temperatures around and exceeding CT_{max} in European perch (*Perca fluviatilis*), which was interpreted as an impaired capacity to oxidize pyruvate, which could ultimately limit the entry of electrons into the ETS (Ekström et al., 2017). However, the literature is ambiguous on the potential limitation of CS (and PDH) on ectotherm metabolism at high temperatures and it has been disputed in mussels (Hraoui et al., 2020). Nevertheless, it must be noted that the enzymatic activity measured *in vitro* here represents the maximal catalytic capacity and that this may not directly reflect metabolic flux *in vivo*. Thus, the temperature mismatch between enzymatic activity and CI-OXPHOS breakdown could suggest involvement of other components of the substrate oxidation system, e.g. the mitochondrial pyruvate carrier. Although the decreased catalytic capacity of CS and PDH activity may create a bottleneck for NADH production by the TCA cycle, this cannot fully explain the drastic drop in CI-OXPHOS observed at high temperatures. A possible explanation would be that allosteric regulation and/or covalent modification occur at the level of CI at high temperature, reducing its ability to oxidize NADH. The present study shows that CI-supported oxygen consumption is challenged at high temperatures across the tested *Drosophila* system, with abrupt declines in CI-OXPHOS at temperatures that correlate with species heat tolerance (Fig. 3A), but also that this decline is not likely to be an effect of heat perturbations on the CI enzyme itself. Instead, the enzymes PDH and CS, which are working downstream of the ETS, showed decreased activity at high temperatures and this may point to a cause of the observed decrease in CI-OXPHOS, i.e. that the substrate oxidation system fails to provide the appropriate amount of NADH to CI.

Mitochondrial flexibility: oxidation of alternative substrates sustains high maximal oxygen consumption rates

Insect species have different preferred substrates for flight metabolism; short-term fliers like flies and bees (*Diptera* and *Hymenoptera*) mainly use carbohydrates while locusts and butterflies (*Orthoptera* and *Lepidoptera*) use fats as fuel for sustained flight (Chadwick and Gilmour, 1940; Krogh and Weis-Fogh, 1951; Sacktor, 1955). A survey of the literature on insect mitochondrial respiration by Soares et al. (2015) indicated that *Drosophila* are particularly reliant on NADH-dependent (i.e. electron donors for CI) respiration, which includes pyruvate, malate and proline. Notice that proline is included as an electron donor for CI as it can be transformed into α-ketoglutarate and thus increase TCA cycle intermediates to oxidize pyruvate (anaplerotic role; Fig. 1) (Sacktor and Childress, 1967). However, proline is also recognized as a direct electron donor to the ubiquinone pool through the flavoenzyme ProDH (Bursell, 1981; McDonald et al., 2018; Olembo and Pearson, 1982; Soares et al., 2015; Teulier et al., 2016), and some insects are even reliant on proline as their main fuel (Bursell, 1963; Teulier et al., 2016). G3P is also an important oxidative substrate for insects, allowing the entry of electrons into the ETS via mtG3PDH, as it is at the intersection of glycolysis, fatty acid degradation and oxidative phosphorylation (McDonald et al., 2018). In insect flight muscle, this reaction is the most important redox cycler (glycerol phosphate shuttle) for maintaining redox balance (NAD^+/NADH) in the cytosol (Sacktor, 1975), attested by *Drosophila* mutants with reduced or absent mtG3PDH displaying debilitated flight ability (Carmon and MacIntyre, 2010; Carmon et al., 2010). However, almost nothing is known about the regulatory mechanisms at the three mitochondrial

loci of metabolic control in insects during temperature changes; namely, the oxidation of pyruvate, proline and G3P.

The oxygen consumption rates measured in the present study in *Drosophila* at benign temperatures also indicate that pyruvate (as NADH-dependent OXPHOS or CI-OXPHOS) was the most efficient fuel for the ETS, congruent with the data compiled by Soares et al. (2015). Once temperature increased and the breakdown in CI-OXPHOS was observed, the SCR of the other provided substrates (proline, succinate and G3P) increased (Fig. 2; Fig. S1), but this is not surprising as the calculation of SCR is based on the OCR achieved by the previous substrate. Hence, we investigated whether the 'new-found' use of alternative substrates with increasing temperature was solely due to the loss of CI-OXPHOS (here labelled the masking effect), or whether the pathways for the alternative substrates were increasingly active because of the higher temperatures. To examine this, we conducted a second set of measurements on permeabilized thoraces with a new SUIT protocol, inhibiting CI with rotenone prior to injection of alternative substrates (proline and G3P) at 34°C (when CI-OXPHOS is not usually compromised) and 42°C (when CI-OXPHOS is 'naturally' reduced). We found that proline and particularly G3P efficiently maintained high rates of oxygen consumption (Fig. S3). Together with the increased values of SCR for proline and G3P at high temperatures, this indicates that a masking effect from CI dominates the apparent contribution of alternative substrates to the OCR, rather than a clear temperature effect on alternative pathways.

To summarize, when CI-OXPHOS is challenged by high temperatures (Fig. 3A), other substrates can be oxidized instead to deliver electrons to the ETS. This switch in substrate maintains a high maximal OCR even at temperatures above those normally considered lethal (Fig. 3B). In model simulations of mitochondrial flexibility in human cardiomyocyte mitochondria with CI deficiency, Zieliński et al. (2016) identified two dominant mechanisms to maintain redox balance. These reactions were the glycerol phosphate shuttle (cytosolic) and the cycle between ProDH and pyrroline-5-carboxylate reductase (mitochondrial). In accordance, it has been shown that reduced pyruvate-supported oxygen consumption in mutant *Drosophila* is associated with a compensating increase by ProDH to mitochondrial respiration (Simard et al., 2020a,b). Similarly, decreased mitochondrial respiration at the level of CI in mutant *Drosophila* was associated with an increase in mitochondrial G3P oxidation, compensating for CI deficiency (Pichaud et al., 2019). Our data suggest that the same reactions are important when CI-OXPHOS is reduced by heat stress in *Drosophila*.

In the model simulations from Zieliński et al. (2016), ATP production was reduced when G3P and proline were used as substrates as these reactions do not contribute directly to the proton gradient (only indirectly through the downstream ubiquinone pool). Considering the failure of CI to support the proton gradient at high temperature, it is possible that the sustained oxygen consumption rates at high temperatures are somewhat decoupled to sustained ATP production rates in *Drosophila*. As an example, it was found in the wrasse *Notolabrus celidotus* that respiration through CI and CII in permeabilized cardiac fibres increased at temperatures above the upper tolerance limit but that the concurrent ATP production rate plummeted, resulting in a lower ATP/O ratio (Iftikar and Hickey, 2013; see also Chung and Schulte, 2020). The decreased ATP/O ratio coincides with the temperature of acute heart failure, emphasizing that sustained high mitochondrial oxygen consumption rates may not necessarily result in efficient energy production. Further studies should therefore investigate whether the characteristic hyperthermic failure of CI-OXPHOS result in insufficient ATP production or whether energy production is well defended at critically high temperatures.

Heat stress also increases the production of reactive oxygen species (ROS), which are normal by-products of cellular respiration and represent both an important signalling molecule and a potential source of cellular injury (Abele et al., 2002; Blier et al., 2014; Scialò et al., 2020). CI is normally considered the main source of ROS (Murphy, 2009) but in *Drosophila*, mtG3PDH is one of the most significant producers of ROS (Miwa and Brand, 2005; Miwa et al., 2003). Investigating ROS production at high temperatures is thus an interesting direction for future studies given the breakdown in CI-OXPHOS, the resulting increase in the relative contribution of mtG3PDH and the sustained high mitochondrial oxygen consumption rates observed here.

In summary, this study shows that mitochondrial oxygen consumption is sustained at temperatures around and above the species heat tolerance limits, indicating that mitochondria may be more tolerant than the animal itself, in accordance with previous studies. In all of the tested species, we observed abrupt declines in the OCR supported by CI substrates, in a pattern that correlates with species heat tolerance. Measurements of enzymatic activity revealed that the CI enzyme alone is unlikely to be responsible for the observed decline in CI-OXPHOS. Instead, upstream enzymes of the substrate oxidation system such as the PDH complex and CS may potentially limit CI-OXPHOS at high temperatures as a result of their decline in activity. Using an alternative SUIT protocol, we also observed that the increased relative reliance on G3P and proline is largely attributable to a masking effect of CI-supported respiration. Hence, mitochondrial oxygen consumption persists even at critically high temperatures through the use of alternative substrates. It is, however, unclear whether this oxygen use is coupled to sufficient energy production. Future studies should include examination of ATP production at high temperatures to investigate whether the high mitochondrial oxygen consumption is coupled to energy production, and further, whether the oxygen consumption in combination with alternative substrate pathways and high temperature can result in increased ROS production, ultimately posing an oxidative stress challenge in *Drosophila* near their upper thermal limit.

Acknowledgements
The authors would like to thank Rebekah Strang and Kirsten Kromand for animal care in Canada and Denmark, respectively, Professors Angela Fago and Tobias Wang for allowing us to use their Oroboros systems at Aarhus University, and Dr Amanda Bundgaard for valuable discussions.

Competing interests
The authors declare no competing or financial interests.

Author contributions
Conceptualization: L.B.J., J.O., N.P.; Methodology: L.B.J., J.O., N.P.; Validation: L.B.J., N.P.; Formal analysis: L.B.J., N.P.; Investigation: L.B.J., F. H.-M., N.P.; Resources: J.O., N.P.; Data curation: L.B.J.; Writing - original draft: L.B.J., J.O., N.P.; Writing - review & editing: L.B.J., J.O., F. H.-M., N.P.; Visualization: L.B.J.; Supervision: L.B.J., J.O., N.P.; Project administration: L.B.J., J.O., N.P.; Funding acquisition: L.B.J., J.O., N.P.

Funding
This research was funded by grants from Université de Moncton (N.P.), the Natural Sciences and Engineering Research Council of Canada (NSERC) (RGPIN-2017-05100) (N.P.), and the Danish Council for Independent Research|Natural Sciences (Det Frie Forskningsråd|Natur og Univers) (J.O.). L.B.J. was supported by a Company of Biologists Travel Fellowship (sponsored by Journal of Experimental Biology, JEBTF1905228).

Data availability
Data are available from Zenodo: https://zenodo.org/record/4556839

Supplementary information

Supplementary information available online at
https://jeb.biologists.org/lookup/doi/10.1242/jeb.240960.supplemental

References

Abele, D., Heise, K., Pörtner, H. O. and Puntarulo, S. (2002). Temperature-dependence of mitochondrial function and production of reactive oxygen species in the intertidal mud clam *Mya arenaria*. *J. Exp. Biol.* **205**, 1831-1841.

Addo-Bediako, A., Chown, S. L. and Gaston, K. J. (2000). Thermal tolerance, climatic variability and latitude. *Proc. Biol. Sci.* **267**, 739-745. doi:10.1098/rspb.2000.1065

Andersen, J. L., Manenti, T., Sørensen, J. G., MacMillan, H. A., Loeschcke, V. and Overgaard, J. (2015). How to assess *Drosophila* cold tolerance: chill coma temperature and lower lethal temperature are the best predictors of cold distribution limits. *Funct. Ecol.* **29**, 55-65. doi:10.1111/1365-2435.12310

Beenakkers, A. M. T., van der Horst, D. J. and Van Marrewijk, W. J. A. (1984). Insect flight muscle metabolism. *Insect Biochem.* **14**, 243-260. doi:10.1016/0020-1790(84)90057-X

Blier, P. U., Lemieux, H. and Pichaud, N. (2014). Holding our breath in our modern world: will mitochondria keep the pace with climate changes? *Can. J. Zool.* **92**, 591-601. doi:10.1139/cjz-2013-0183

Bowler, K. (2018). Heat death in poikilotherms: Is there a common cause? *J. Therm. Biol.* **76**, 77-79. doi:10.1016/j.jtherbio.2018.06.007

Bowler, K. and Kashmeery, A. M. S. (1979). Recovery from heat injury in the blowfly, *Calliphora erythrocephala*. *J. Therm. Biol.* **4**, 197-202. doi:10.1016/0306-4565(79)90001-9

Bowler, K. and Kashmeery, A. M. S. (1981). Effects of *in vivo* heating of blowflies on the oxidative capacity of flight muscle sarcosomes: a differential effect on glycerol 3-phosphate and pyruvate plus proline respiration. *J. Therm. Biol.* **6**, 11-18. doi:10.1016/0306-4565(81)90036-X

Bursell, E. (1963). Aspects of the metabolism of amino acids in the tsetse fly, *Glossina* (Diptera). *J. Insect Physiol.* **9**, 439-452. doi:10.1016/0022-1910(63)90054-4

Bursell, E. (1981). The role of proline in energy metabolism. In *Energy Metabolism in Insects* (ed. R. G. H. Downer), pp. 135-154. Boston, MA: Springer.

Candy, D. J., Becker, A. and Wegener, G. (1997). Coordination and integration of metabolism in insect flight. *Comp. Biochem. Physiol. B Biochem. Mol. Biol.* **117**, 497-512. doi:10.1016/S0305-0491(97)00212-5

Carmon, A. and MacIntyre, R. (2010). The α glycerophosphate cycle in *Drosophila melanogaster* VI. structure and evolution of enzyme paralogs in the genus *Drosophila*. *J. Hered.* **101**, 225-234. doi:10.1093/jhered/esp111

Carmon, A., Chien, J., Sullivan, D. and MacIntyre, R. (2010). The α glycerophosphate cycle in *Drosophila melanogaster* V. Molecular analysis of α glycerophosphate dehydrogenase and α glycerophosphate oxidase mutants. *J. Hered.* **101**, 218-224. doi:10.1093/jhered/esp110

Chadwick, L. E. and Gilmour, D. (1940). Respiration during flight in *Drosophila repleta* Wollaston: the oxygen consumption considered in relation to the wing-rate. *Physiol. Zool.* **13**, 398-410. doi:10.1086/physzool.13.4.30151588

Chamberlin, M. E. (2004). Top-down control analysis of the effect of temperature on ectotherm oxidative phosphorylation. *Am. J. Physiol. Regul. Integr. Comp. Physiol.* **287**, R794-R800. doi:10.1152/ajpregu.00240.2004

Chung, D. J. and Schulte, P. M. (2020). Mitochondria and the thermal limits of ectotherms. *J. Exp. Biol.* **223**, jeb227801. doi:10.1242/jeb.227801

Chung, D. J., Sparagna, G. C., Chicco, A. J. and Schulte, P. M. (2018). Patterns of mitochondrial membrane remodeling parallel functional adaptations to thermal stress. *J. Exp. Biol.* **221**, jeb174458. doi:10.1242/jeb.174458

Cormier, R. P. J., Champigny, C. M., Simard, C. J., St-Coeur, P. D. and Pichaud, N. (2019). Dynamic mitochondrial responses to a high-fat diet in *Drosophila melanogaster*. *Sci. Rep.* **9**, 1-11. doi:10.1038/s41598-018-36060-5

Dahlhoff, E. and Somero, G. N. (1993). Kinetic and structural adaptations of cytoplasmic malate dehydrogenases of eastern Pacific abalone (genus *Haliotis*) from different thermal habitats: biochemical correlates of biogeographical patterning. *J. Exp. Biol.* **185**, 137-150.

Davis, B. Y. R. A. and Fraenkel, G. (1940). The oxygen consumption of flies during flight. *J. Exp. Biol.* **17**, 402-407.

Davison, T. F. and Bowler, K. (1971). Changes in the functional efficiency of flight muscle sarcosomes during heat death of adult *Calliphora erythrocephala*. *J. Cell. Physiol.* **78**, 37-47. doi:10.1002/jcp.1040780107

Ekström, A., Sandblom, E., Blier, P. U., Dupont Cyr, B.-A., Brijs, J. and Pichaud, N. (2017). Thermal sensitivity and phenotypic plasticity of cardiac mitochondrial metabolism in European perch, *Perca fluviatilis*. *J. Exp. Biol.* **220**, 386-396. doi:10.1242/jeb.150698

El-Wadawi, R. and Bowler, K. (1995). The development of thermotolerance protects blowfly flight muscle mitochondrial function from heat damage. *J. Exp. Biol.* **198**, 2413-2421.

El-Wadawi, R. and Bowler, K. (1996). The effect of *in vivo* heat treatments on blowfly flight muscle mitochondrial function: Effects on partial reactions of the respiratory chain. *J. Therm. Biol.* **21**, 403-408. doi:10.1016/S0306-4565(96)00024-1

Fangue, N. A., Richards, J. G. and Schulte, P. M. (2009). Do mitochondrial properties explain intraspecific variation in thermal tolerance? *J. Exp. Biol.* **212**, 514-522. doi:10.1242/jeb.024034

Gnaiger, E. (2014). *Mitochondrial Pathways and Respiratory Control. An Introduction to OXPHOS Analysis*, 4th edn., pp. 1-80. Innsbruck, Austria: OROBOROS MiPNet Publications.

González-Tokman, D., Córdoba-Aguilar, A., Dáttilo, W., Lira-Noriega, A., Sánchez-Guillén, R. A. and Villalobos, F. (2020). Insect responses to heat: physiological mechanisms, evolution and ecological implications in a warming world. *Biol. Rev.* **95**, 802-821. doi:10.1111/brv.12588

Harada, A. E., Healy, T. M. and Burton, R. S. (2019). Variation in thermal tolerance and its relationship to mitochondrial function across populations of *Tigriopus californicus*. *Front. Physiol.* **10**. doi:10.3389/fphys.2019.00213

Havird, J. C., Shah, A. A. and Chicco, A. J. (2020). Powerhouses in the cold: mitochondrial function during thermal acclimation in montane mayflies. *Philos. Trans. R. Soc. Lond. B. Biol. Sci.* **375**, 20190181. doi:10.1098/rstb.2019.0181

Heinrich, E. C., Gray, E. M., Ossher, A., Meigher, S., Grun, F. and Bradley, T. J. (2017). Aerobic function in mitochondria persists beyond death by heat stress in insects. *J. Therm. Biol.* **69**, 267-274. doi:10.1016/j.jtherbio.2017.08.009

Hilton, Z., Clements, K. D. and Hickey, A. J. R. (2010). Temperature sensitivity of cardiac mitochondria in intertidal and subtidal triplefin fishes. *J. Comp. Physiol. B* **180**, 979-990. doi:10.1007/s00360-010-0477-7

Hirst, J. (2010). Towards the molecular mechanism of respiratory complex I. *Biochem. J.* **425**, 327-339. doi:10.1042/BJ20091382

Hochachka, P. W. and Somero, G. N. (2002). *Biochemical Adaptation: Mechanism and Process in Physiological Evolution*. New York: Oxford University Press.

Hraoui, G., Bettinazzi, S., Gendron, A. D., Boisclair, D. and Breton, S. (2020). Mitochondrial thermo-sensitivity in invasive and native freshwater mussels. *J. Exp. Biol.* **223**, jeb215921. doi:10.1242/jeb.215921

Hunter-Manseau, F., Desrosiers, V., Le François, N. R., Dufresne, F., Detrich, H. W., , III, Nozais, C. and Blier, P. U. (2019). From Africa to Antarctica: exploring the metabolism of fish heart mitochondria across a wide thermal range. *Front. Physiol.* **10**. doi:10.3389/fphys.2019.01220

Iftikar, F. I. and Hickey, A. J. R. (2013). Do Mitochondria Limit Hot Fish Hearts? Understanding the Role of Mitochondrial Function with Heat Stress in *Notolabrus celidotus*. *PLoS One* **8**, e64120. doi:10.1371/journal.pone.0064120

Iftikar, F. I., MacDonald, J. and Hickey, A. J. R. (2010). Thermal limits of portunid crab heart mitochondria: Could more thermo-stable mitochondria advantage invasive species? *J. Exp. Mar. Bio. Ecol.* **395**, 232-239. doi:10.1016/j.jembe.2010.09.005

Iftikar, F. I., MacDonald, J. R., Baker, D. W., Renshaw, G. M. C. and Hickey, A. J. R. (2014). Could thermal sensitivity of mitochondria determine species distribution in a changing climate? *J. Exp. Biol.* **217**, 2348-2357. doi:10.1242/jeb.098798

IPCC. (2014). *Climate Change 2014: Synthesis Report. Contribution of Working Groups I, II and III to the Fifth Assessment Report of the Intergovernmental Panel on Climate Change* (ed. **Core Writing Team**, R. K. Pachauri and L. A. Meyer). Geneva, Switzerland: IPCC.

Jørgensen, L. B., Malte, H. and Overgaard, J. (2019). How to assess *Drosophila* heat tolerance: unifying static and dynamic tolerance assays to predict heat distribution limits. *Funct. Ecol.* **33**, 629-642. doi:10.1111/1365-2435.13279

Kake-Guena, S. A., Touisse, K., Warren, B. E., Scott, K. Y., Dufresne, F., Blier, P. U. and Lemieux, H. (2017). Temperature-related differences in mitochondrial function among clones of the cladoceran *Daphnia pulex*. *J. Therm. Biol.* **69**, 23-31. doi:10.1016/j.jtherbio.2017.05.005

Kellermann, V., Overgaard, J., Hoffmann, A. A., Fløjgaard, C., Svenning, J.-C. and Loeschcke, V. (2012). Upper thermal limits of *Drosophila* are linked to species distributions and strongly constrained phylogenetically. *Proc. Natl. Acad. Sci. USA* **109**, 16228-16233. doi:10.1073/pnas.1207553109

Kingsolver, J. G., Diamond, S. E. and Buckley, L. B. (2013). Heat stress and the fitness consequences of climate change for terrestrial ectotherms. *Funct. Ecol.* **27**, 1415-1423. doi:10.1111/1365-2435.12145

Klok, C. J. (2004). Upper thermal tolerance and oxygen limitation in terrestrial arthropods. *J. Exp. Biol.* **207**, 2361-2370. doi:10.1242/jeb.01023

Kovac, H., Käfer, H., Stabentheiner, A. and Costa, C. (2014). Metabolism and upper thermal limits of *Apis mellifera carnica* and *A. m. ligustica*. *Apidologie* **45**, 664-677. doi:10.1007/s13592-014-0284-3

Krogh, A. and Weis-Fogh, T. (1951). The respiratory exchange of the desert locust (*Schistocerca gregaria*) before, during and after flight. *J. Exp. Biol.* **28**, 344-357.

Kuznetsov, A. V., Veksler, V., Gellerich, F. N., Saks, V., Margreiter, R. and Kunz, W. S. (2008). Analysis of mitochondrial function *in situ* in permeabilized muscle fibers, tissues and cells. *Nat. Protoc.* **3**, 965-976. doi:10.1038/nprot.2008.61

Lemieux, H., Tardif, J.-C. and Blier, P. U. (2010a). Thermal sensitivity of oxidative phosphorylation in rat heart mitochondria: Does pyruvate dehydrogenase dictate the response to temperature? *J. Therm. Biol.* **35**, 105-111. doi:10.1016/j.jtherbio.2009.12.003

Lemieux, H., Tardif, J.-C., Dutil, J.-D. and Blier, P. U. (2010b). Thermal sensitivity of cardiac mitochondrial metabolism in an ectothermic species from a cold environment, Atlantic wolffish (*Anarhichas lupus*). *J. Exp. Mar. Bio. Ecol.* **384**, 113-118. doi:10.1016/j.jembe.2009.12.007

Martinez, E., Hendricks, E., Menze, M. A. and Torres, J. J. (2016). Physiological performance of warm-adapted marine ectotherms: thermal limits of mitochondrial energy transduction efficiency. *Comp. Biochem. Physiol. A Mol. Integr. Physiol.* **191**, 216-225. doi:10.1016/j.cbpa.2015.08.008

McDonald, A. E., Pichaud, N. and Darveau, C.-A. (2018). "Alternative" fuels contributing to mitochondrial electron transport: importance of non-classical pathways in the diversity of animal metabolism. *Comp. Biochem. Physiol. B Biochem. Mol. Biol.* **224**, 185-194. doi:10.1016/j.cbpb.2017.11.006

Miwa, S. and Brand, M. D. (2005). The topology of superoxide production by complex III and glycerol 3-phosphate dehydrogenase in *Drosophila* mitochondria. *Biochim. Biophys. Acta Bioenerg.* **1709**, 214-219. doi:10.1016/j.bbabio.2005.08.003

Miwa, S., St-Pierre, J., Partridge, L. and Brand, M. D. (2003). Superoxide and hydrogen peroxide production by *Drosophila* mitochondria. *Free Radic. Biol. Med.* **35**, 938-948. doi:10.1016/S0891-5849(03)00464-7

Mölich, A. B., Förster, T. D. and Lighton, J. R. B. (2013). Hyperthermic overdrive: oxygen delivery does not limit thermal tolerance in *Drosophila melanogaster*. *J. Insect Sci.* **12**, 1-7. doi:10.1673/031.012.10901

Murphy, M. P. (2009). How mitochondria produce reactive oxygen species. *Biochem. J.* **417**, 1-13. doi:10.1042/BJ20081386

Neven, L. G. (2000). Physiological responses of insects to heat. *Postharvest Biol. Technol.* **21**, 103-111. doi:10.1016/S0925-5214(00)00169-1

Olembo, N. K. and Pearson, D. J. (1982). Changes in the contents of intermediates of proline and carbohydrate metabolism in flight muscle of the tsetse fly *Glossina morsitans* and the fleshfly *Sarcophaga tibialis*. *Insect Biochem.* **12**, 657-662. doi:10.1016/0020-1790(82)90053-1

Pichaud, N., Chatelain, E. H., Ballard, J. W. O., Tanguay, R., Morrow, G. and Blier, P. U. (2010). Thermal sensitivity of mitochondrial metabolism in two distinct mitotypes of *Drosophila simulans*: evaluation of mitochondrial plasticity. *J. Exp. Biol.* **213**, 1665-1675. doi:10.1242/jeb.040261

Pichaud, N., Ballard, J. W. O., Tanguay, R. M. and Blier, P. U. (2011). Thermal sensitivity of mitochondrial functions in permeabilized muscle fibers from two populations of *Drosophila simulans* with divergent mitotypes. *Am. J. Physiol. Regul. Integr. Comp. Physiol.* **301**, R48-R59. doi:10.1152/ajpregu.00542.2010

Pichaud, N., Ballard, J. W. O., Tanguay, R. M. and Blier, P. U. (2012). Naturally occurring mitochondrial DNA haplotypes exhibit metabolic differences: insight into functional properties of mitochondria. *Evolution (N. Y).* **66**, 3189-3197. doi:10.1111/j.1558-5646.2012.01683.x

Pichaud, N., Ballard, J. W. O., Tanguay, R. M. and Blier, P. U. (2013). Mitochondrial haplotype divergences affect specific temperature sensitivity of mitochondrial respiration. *J. Bioenerg. Biomembr.* **45**, 25-35. doi:10.1007/s10863-012-9473-9

Pichaud, N., Bérubé, R., Côté, G., Belzile, C., Dufresne, F., Morrow, G., Tanguay, R. M., Rand, D. M. and Blier, P. U. (2019). Age dependent dysfunction of mitochondrial and ROS metabolism induced by mitonuclear mismatch. *Front. Genet.* **10**, 1-12. doi:10.3389/fgene.2019.00130

Pobezhimova, T., Voinikov, V. and Varakina, N. (1996). Inactivation of complex I of the respiratory chain of maize mitochondria incubated *in vitro* by elevated temperature. *J. Therm. Biol.* **21**, 283-288. doi:10.1016/S0306-4565(96)00010-1

Riddles, P. W., Blakeley, R. L. and Zerner, B. (1979). Ellman's reagent: 5,5′-dithiobis(2-nitrobenzoic acid) - a reexamination. *Anal. Biochem.* **94**, 75-81. doi:10.1016/0003-2697(79)90792-9

Sacktor, B. (1955). Cell structure and the metabolism of insect flight muscle. *J. Biophys. Biochem. Cytol.* **1**, 29-46. doi:10.1083/jcb.1.1.29

Sacktor, B. (1975). Biochemistry of insect flight. In *Insect Biochemistry and Function* (ed. D. J. Candy and B. A. Kilby), pp. 89-176. London: Chapman and Hall.

Sacktor, B. and Childress, C. C. (1967). Metabolism of proline in insect flight muscle and its significance in stimulating the oxidation of pyruvate. *Arch. Biochem. Biophys.* **120**, 583-588. doi:10.1016/0003-9861(67)90522-X

Schmidt-Nielsen, K. (1990). *Animal Physiology: Adaptation and Environment*, 4th edn. Cambridge: Cambridge University Press.

Schulte, P. M. (2015). The effects of temperature on aerobic metabolism: towards a mechanistic understanding of the responses of ectotherms to a changing environment. *J. Exp. Biol.* **218**, 1856-1866. doi:10.1242/jeb.118851

Scialò, F., Sriram, A., Stefanatos, R., Spriggs, R. V., Loh, S. H. Y., Martins, L. M. and Sanz, A. (2020). Mitochondrial complex I derived ROS regulate stress adaptation in *Drosophila melanogaster*. *Redox Biol.* **32**, 101450. doi:10.1016/j.redox.2020.101450

Simard, C. J., Pelletier, G., Boudreau, L. H., Hebert-chatelain, E. and Pichaud, N. (2018). Measurement of mitochondrial oxygen consumption in permeabilized fibers of *Drosophila* using minimal amounts of tissue. *J. Vis. Exp.* **134**, e57376. doi:10.3791/57376

Simard, C. J., Touaibia, M., Allain, E. P., Hebert-Chatelain, E. and Pichaud, N. (2020a). Role of the mitochondrial pyruvate carrier in the occurrence of metabolic inflexibility in *Drosophila melanogaster* exposed to dietary sucrose. *Metabolites* **10**, 411. doi:10.3390/metabo10100411

Simard, C., Lebel, A., Allain, E. P., Touaibia, M., Hebert-Chatelain, E. and Pichaud, N. (2020b). Metabolic characterization and consequences of mitochondrial pyruvate carrier deficiency in *Drosophila melanogaster*. *Metabolites* **10**, 363. doi:10.3390/metabo10090363

Smith, P. K., Krohn, R. I., Hermanson, G. T., Mallia, A. K., Gartner, F. H., Provenzano, M. D., Fujimoto, E. K., Goeke, N. M., Olson, B. J. and Klenk, D. C. (1985). Measurement of protein using bicinchoninic acid. *Anal. Biochem.* **150**, 76-85. doi:10.1016/0003-2697(85)90442-7

Soares, J. B. R. C., Gaviraghi, A. and Oliveira, M. F. (2015). Mitochondrial physiology in the major arbovirus vector *Aedes aegypti*: substrate preferences and sexual differences define respiratory capacity and superoxide production. *PLoS ONE* **10**, e0120600. doi:10.1371/journal.pone.0120600

Stork, N. E. (2018). How many species of insects and other terrestrial arthropods are there on earth? *Annu. Rev. Entomol.* **63**, 31-45. doi:10.1146/annurev-ento-020117-043348

Sunday, J. M., Bates, A. E. and Dulvy, N. K. (2012). Thermal tolerance and the global redistribution of animals. *Nat. Clim. Chang.* **2**, 686-690. doi:10.1038/nclimate1539

Sunday, J., Bennett, J. M., Calosi, P., Clusella-Trullas, S., Gravel, S., Hargreaves, A. L., Leiva, F. P., Verberk, W. C. E. P., Olalla-Tárraga, M. Á. and Morales-Castilla, I. (2019). Thermal tolerance patterns across latitude and elevation. *Philos. Trans. R. Soc. B Biol. Sci.* **374**, 20190036. doi:10.1098/rstb.2019.0036

Syromyatnikov, M. Y., Gureev, A. P., Vitkalova, I. Y., Starkov, A. A. and Popov, V. N. (2019). Unique features of flight muscles mitochondria of honey bees (*Apis mellifera* L.). *Arch. Insect Biochem. Physiol.* **102**, 1-14. doi:10.1002/arch.21595

Teulier, L., Weber, J.-M., Crevier, J. and Darveau, C.-A. (2016). Proline as a fuel for insect flight: enhancing carbohydrate oxidation in hymenopterans. *Proc. R. Soc. B Biol. Sci.* **283**. doi:10.1098/rspb.2016.0333

Verberk, W. C. E. P., Overgaard, J., Ern, R., Bayley, M., Wang, T., Boardman, L. and Terblanche, J. S. (2015). Does oxygen limit thermal tolerance in arthropods? A critical review of current evidence. *Comp. Biochem. Physiol. A. Mol. Integr. Physiol.* **192**, 64-78. doi:10.1016/j.cbpa.2015.10.020

Weis-Fogh, T. (1964). Diffusion in insect wing muscle, the most active tissue known. *J. Exp. Biol.* **41**, 229-256.

Zieliński, Ł. P., Smith, A. C., Smith, A. G. and Robinson, A. J. (2016). Metabolic flexibility of mitochondrial respiratory chain disorders predicted by computer modelling. *Mitochondrion* **31**, 45-55. doi:10.1016/j.mito.2016.09.003